

# Influence of both Calcining and Sintering Temperature on the Structural Characteristics of Cobalt Ferrite Material

Sabah H. Sabeeh and Zahraa S. Ahmed

**Abstract**— In this work the Nano-magnetic materials (cobalt ferrite) with formula ( $\text{CoFe}_2\text{O}_4$ ) as nano-powder was prepared from (Ferric Nitrite, Cobalt Nitrite and Citric Acid) by utilizing sol-gel auto combustion method, with different pH (3, 5, and 7), then the powder were calcined at different temperatures (300, 500, and 700) $^\circ\text{C}$ , and the samples sintered at different temperatures (1000, and 1100) $^\circ\text{C}$ . The structural properties (X-Ray Diffraction [XRD], SEM, EDS, and AFM) of these samples were studied. All samples exhibit similar diffraction peaks which correspond to the cubic spinel lattice of  $\text{CoFe}_2\text{O}_4$ , the products contained spherical particles but to some extent aggregations were observed in each sample. The (SEM) images show that the average particles size decreases when the calcining temperatures increase, this occurs due to the temperature that affects only the radius of nanoparticles, except the samples with (pH = 5). It is clear that Co: Fe ratio is 1:2 indicating that the stoichiometric proportion is used, which lead to prove the Co: Fe ratio is maintained. The images of (AFM) showed that a uniform structure without any valleys was observed and all the particles are aligned vertically due to the homogenous distribution of the ferrite particles.

**Index Terms**— Cobalt ferrite, Nano-magnetic material, Sol-gel auto-combustion, Spinel ferrite structure.

## 1 INTRODUCTION

FERRITE nanoparticles are important magnetic materials due to their specific properties and the relationships between their magnetic properties and their crystal chemistry and structure, which lead to broaden their applications [1-3]. Various methods have been developed for the synthesis of nano ferrites, like sono- chemical reactions, sol-gel, microwave plasma, co precipitation, micro emulsion and chemical vapour deposition etc.

Cobalt ferrite is an attractive material due to its unique optical, electronic, magnetic properties, excellent chemical stability, mechanical hardness, large anisotropy, high coercivity, high Currie temperature and high saturation magnetization [4, 5]. High coercivity gives cobalt ferrite potential in high-capacity magnetic storage, whereas high magnetic anisotropy forces the particles to relax through the Brownian mechanism, giving them potential applications as sensors [6]. Therefore, it is a promising choice for high density magnetic recording, Ferro fluids technology, bio-molecule separation, biomedical drug delivery, catalysis, magnetic resonance imaging, biocompatible magnetic nano-particles for cancer treatment and magneto-optical devices. It is well known that magnetic properties depend also on the size, morphology and purity of ferrite particles. Therefore, the choice of preparation method plays key role in the observation of fine product with excellent properties. So that there are various methods to obtain cobalt ferrite nanoparticles, such as mechanical, thermal decomposition, sol-gel method, chemical co-precipitation, mechanochemical processing, hydrothermal, sol-gel auto-combustion, and microemulsion method [4]. The crystallite size is determined by utilizing the Scherrer' equation:

$$D = \frac{0.9\lambda}{\beta \cos \theta} \quad (1)$$

where  $\lambda$  is the wavelength of X-ray used,  $\theta$  is the Bragg's angle,  $\beta$  is the full width at half maximum (FWHM) in radian.

The X-ray density ( $\rho_x$ ) is calculated by using the formula:

$$\rho_x = \frac{8M}{Na^3} \quad (2)$$

where ( $M$ ) is the molecular weight of the samples, ( $N$ ) is the Avogadro number, ( $a$ ) is the lattice constant and ( $8$ ) stands for the number of formula units in a unit cell.

The lattice constant ( $a$ ) is calculated using the relation:

$$a = d_{hkl} (h^2 + k^2 + l^2)^{1/2} \quad (3)$$

where ( $h, k, l$ ) are the Miller indices of the crystal planes and ( $d_{hkl}$ ) is the inter planer spacing[7].

Zhenfa et al. [8]; prepared  $\text{CoFe}_2\text{O}_4$  ferrite nanoparticles by a modified chemical co-precipitation route. Structural and magnetic properties were systematically investigated. X-ray diffraction results showed that the sample was in single pure phase. The results of field-emission scanning electronic microscopy show that the grains appear spherical with diameters ranging from (20 to 30) nm. The composition was determined by energy-dispersive spectroscopy with stoichiometry of  $\text{CoFe}_2\text{O}_4$ .

VLAZAN, and VASILE [9]; prepared nano-crystalline particles of  $\text{CoFe}_2\text{O}_4$  with a spinel structure by hydrothermal method. The synthesized nanoparticles were characterized by XRD, SEM, and AFM techniques. XRD analysis revealed a high degree of crystallinity and also indicated that the diffraction peaks correspond to the cubic spinel structure. The morphology of the obtained powders was studied by SEM technique; the obtained SEM images evidenced the presence of spherical

nanometric scale ferrite particles. The AFM data for  $\text{CoFe}_2\text{O}_4$  showed a uniform surface; the average grain size estimated from AFM data was  $\sim (40)$  nm.

**Sajjia et al. [10]**; focused on the development of a method to make nano cobalt ferrite powder by using a sol-gel process. Several samples of cobalt ferrite powder were obtained by varying the initial parameters of the process in addition to the heat treatment temperature. X Ray Diffraction and Scanning Electron Microscopy (SEM) were used to identify the structure and morphology of samples demonstrating the influence of the initial parameters. The average particle size, as estimated for one sample by the Full Width at Half Maximum (FWHM) of the strongest X-Ray Diffraction (XRD) peak, was found to be about (45) nm.

**Madani et al. [11]**; produced Cobalt ferrite ( $\text{CoFe}_2\text{O}_4$ ) powders in nano crystalline sizes by a combination of sol-gel auto-combustion and ultrasonic irradiation methods employing a mixture of urea, thiourea and glycine as the fuel with the corresponding metal nitrates. They showed the affecting of pH on the starting solution of the combustion process, so that an increase in the pH value, the combustion rate is increased significantly, and then they determined the particle size of the synthesized powder. The influence of the pH value on the gel auto-combustion and the phase composition of the synthesized powders have been studied with the help of Scanning Electron Microscopy (SEM) observations, Fourier Transform Infrared (FTIR) spectroscopy and X-Ray Diffraction (XRD) techniques. The synthesized powders had a particle size distribution in the range of (23-43) nm, and all the samples are single phase ferrites ( $\text{CoFe}_2\text{O}_4$ ) with cubic spinel structures.

**Shinde [7]**; obtained Cobalt ferrite nano-powders by sol-gel auto-combustion method using citric acid as a fuel. In this method metal nitrate to citric acid ratio was taken as (1:3). The structural characterization of cobalt ferrite nanoparticles was done by X-ray diffraction technique, and the micro-structural and morphological studies were carried out by scanning electron microscope technique and energy dispersive spectrum. The average crystallite size obtained by Scherrer's formula is of the order of (34) nm, and the grain size and specific surface area of the cobalt ferrite nanoparticles was (34 nm and 55nm) respectively.

**Kumar et al. [12]**; prepared the nano-crystalline  $\text{CoFe}_2\text{O}_4$  by nitrate route at the sintering temperature of (300, 500, 700 and 900) °C. The X-Ray Diffraction (XRD) patterns of all the samples showed the single phase spinel structure of nanoparticles. The crystallite sizes varied from (9 to 61) nm as the sintering temperature increases from (300 to 900) °C.

## 2 THE EXPERIMENTAL WORK

### 2.1 Materials

Cobalt (II) nitrate [ $\text{Co}(\text{NO}_3)_2 \cdot 6\text{H}_2\text{O}$  (hexahydrate) 97% puri-

ty, India], ferric (III) nitrate [ $(\text{Fe}(\text{NO}_3)_3 \cdot 9\text{H}_2\text{O})$ , 98% purity, India], citric acid [ $(\text{C}_6\text{H}_8\text{O}_7 \cdot \text{H}_2\text{O})$ , 99% purity, Iraq, Baghdad], distilled water and ammonia solution [ $(\text{NH}_3)$ , India].

### 2.2 Preparation method

The stoichiometric amounts of cobalt (II) nitrate  $\text{Co}(\text{NO}_3)_2 \cdot 6\text{H}_2\text{O}$  and ferric (III) nitrate ( $\text{Fe}(\text{NO}_3)_3 \cdot 9\text{H}_2\text{O}$ ) with ratio 1:2 were dissolved in distilled water under magnetic stirring. Then citric acid ( $\text{C}_6\text{H}_8\text{O}_7 \cdot \text{H}_2\text{O}$ ) was dissolved in distilled water under magnetic stirring and it mixed in the metal nitrate solution to chelate  $\text{Co}^{2+}$  and  $\text{Fe}^{3+}$  ions in the solution. A small amount of ammonia was added drop-wise into the solution to stabilize the nitrate-citrate solution, and then the solution was heated to dryness on a hot plate without stirring until it becomes viscous and finally formed a very viscous gel when temperature becomes (85-95) °C. The temperature is further raised up to 115°C so that the ignition of the gel starts. The dried gel burnt completely in a self-propagating combustion manner to form a loose powder, that it occurs during at one hour. Finally the as burnt powders were calcined in a furnace at different temperatures (300, 500,700) °C for 4 hrs with a heating rate of (10°C / min). After that the samples were sintering at different temperatures (1000,1100)°C for (4)hours with raising rate (10 °C/min) by using furnace with type (Nabertherm) , to get the good samples for studying the properties.

## 3 MEATUREMENTS

The structural characterization was carried out by (X-Ray Diffraction-meter system) type (ADX-2500) , Japan made to prove the composition structure of the produced powder, phases analysis was done by X-Ray Diffraction (XRD) utilizing  $\text{Cu-K}\alpha$  irradiation, and by wavelength  $\lambda = 1.54060 \text{ \AA}$ . by using a device Scanning Electron Microscope (SEM) of (INSPECTS 50) of the type (FEI customer ownership system SN:9922650,Germany) and then was determining the grain size of the prepared powders , as well as the structural and surface morphology, also determined chemical composition of the powder prepared were focused out by using this device , and the average particle size for  $\text{CoFe}_2\text{O}_4$  powder was determined by Atomic Force Microscope (Scanning Probe Microscope (SPM)with type (Angstrom Advanced Inc.,USA) .

## 4 RESULT AND DISCUSSION (STRUCTURAL PROPERTIES)

### 4.1 X-Ray Analysis (XRD)

The XRD patterns of cobalt ferrite ( $\text{CoFe}_2\text{O}_4$ ) nano-particles powder , prepared by this method with different pH , calcined and sintered at different temperatures are shown in Figs (1, 2, 3, 4, 5, 6, 7, 8and 9).

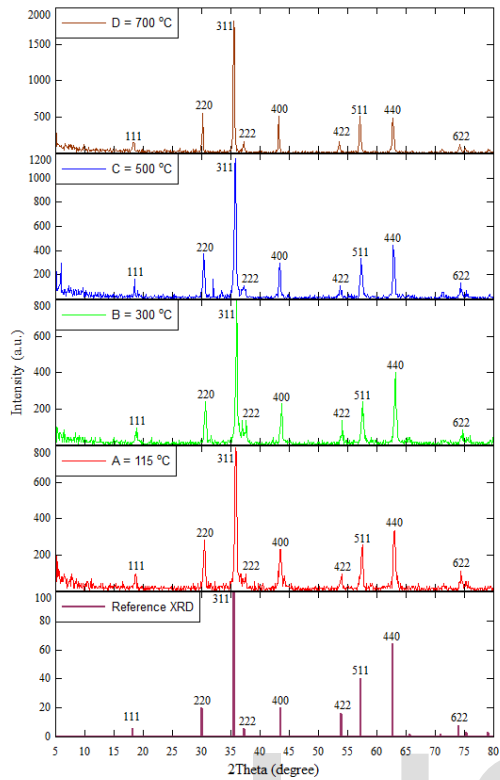


Fig. 1. X-ray diffraction pattern for CoFe<sub>2</sub>O<sub>4</sub> nanoparticles at pH = 3, at different calcining temperatures.

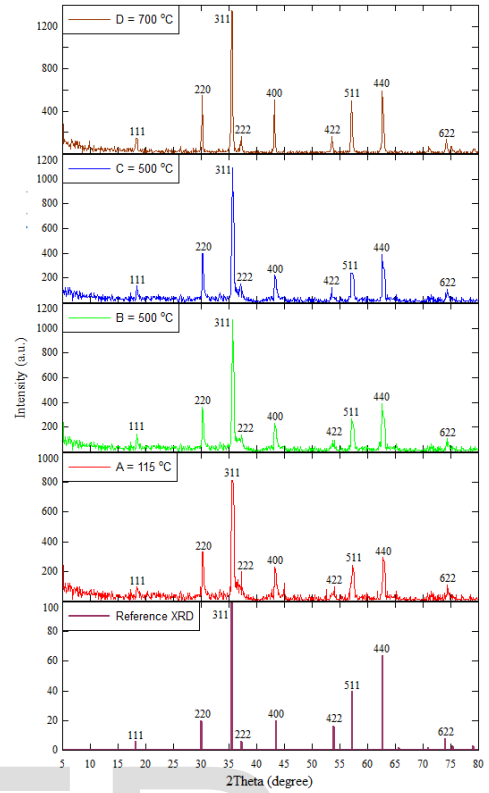


Fig. 3. X-ray diffraction pattern for CoFe<sub>2</sub>O<sub>4</sub> nanoparticles at pH = 7, at different calcining temperatures.

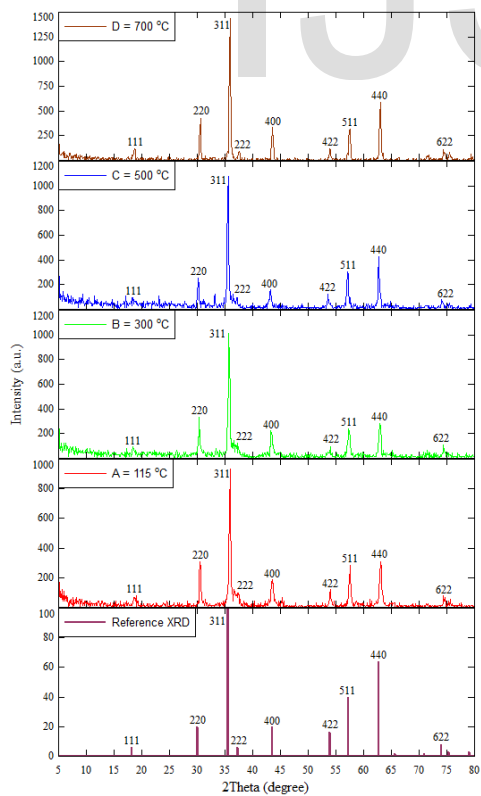


Fig. 2. X-ray diffraction pattern for CoFe<sub>2</sub>O<sub>4</sub> nanoparticles at pH = 5, at different calcining temperatures.

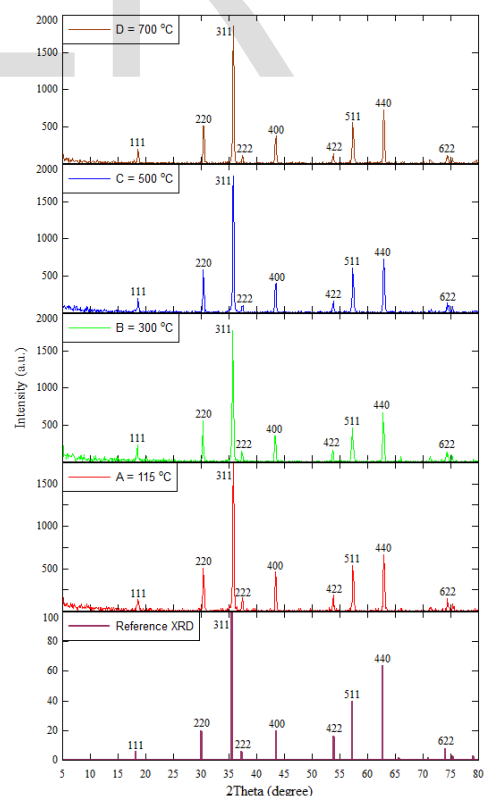


Fig. 4. X-ray diffraction pattern for CoFe<sub>2</sub>O<sub>4</sub> nanoparticles at pH = 3, T<sub>s</sub> = 1000 °C, at different calcining temperatures.

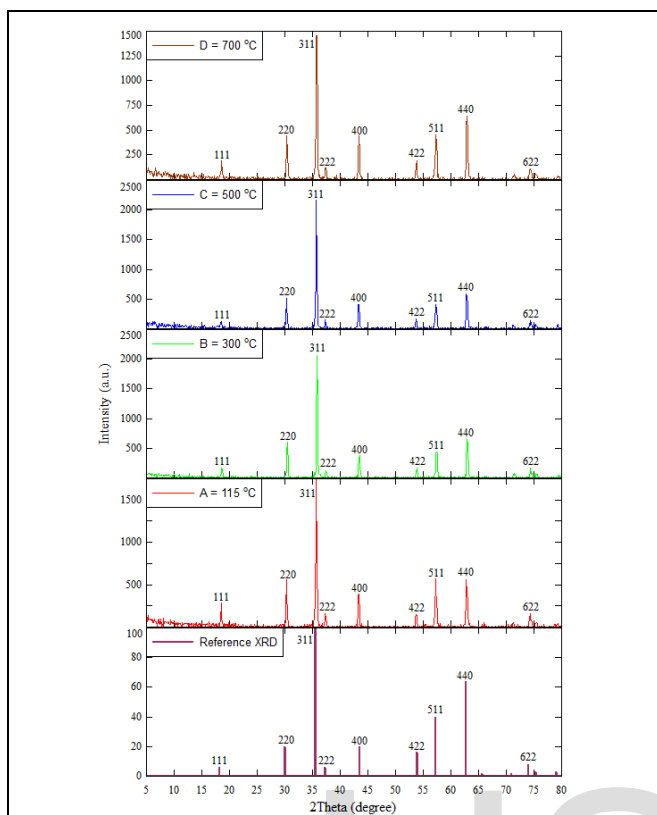


Fig. 5. X-ray diffraction pattern for CoFe<sub>2</sub>O<sub>4</sub> nanoparticles at pH = 5, T<sub>s</sub> = 1000°C, at different calcining temperatures.

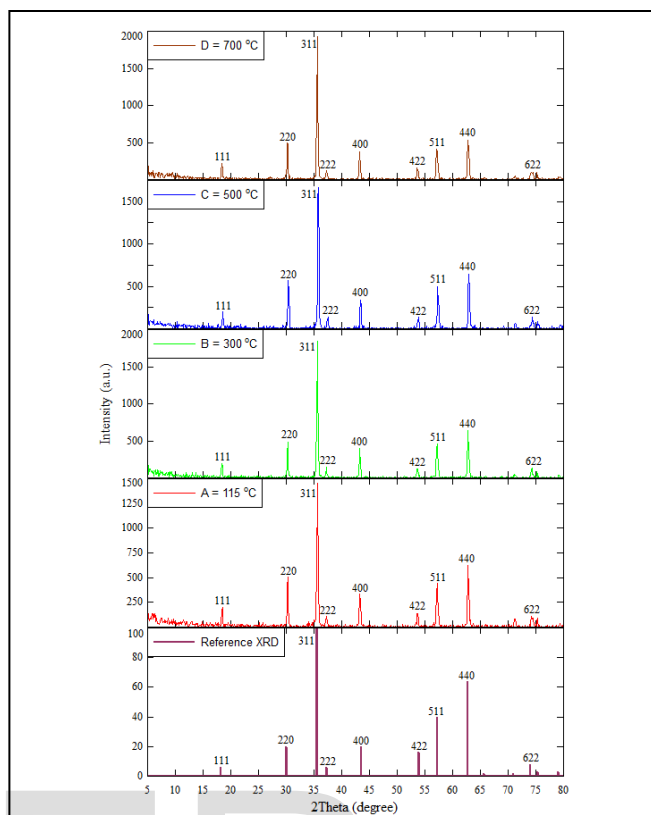


Fig. 7. X-ray diffraction pattern for CoFe<sub>2</sub>O<sub>4</sub> nanoparticles at pH = 3, T<sub>s</sub> = 1100°C, at different calcining temperatures.

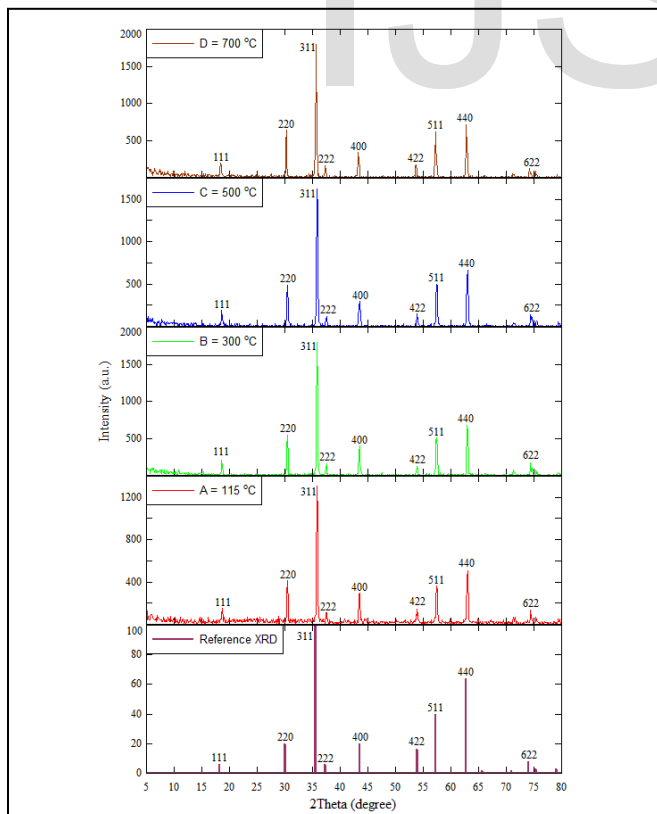


Fig. 6. X-ray diffraction pattern for CoFe<sub>2</sub>O<sub>4</sub> nanoparticles at pH = 7, T<sub>s</sub> = 1000°C, at different calcining temperatures.

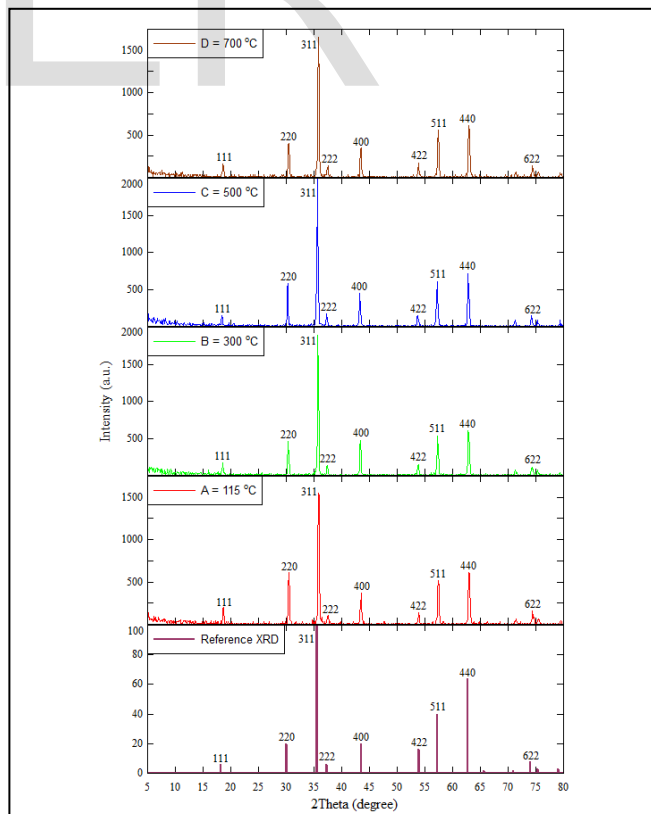


Fig. 9. X-ray diffraction pattern for CoFe<sub>2</sub>O<sub>4</sub> nanoparticles at pH = 5, T<sub>s</sub> = 1100°C, at different calcining temperatures.

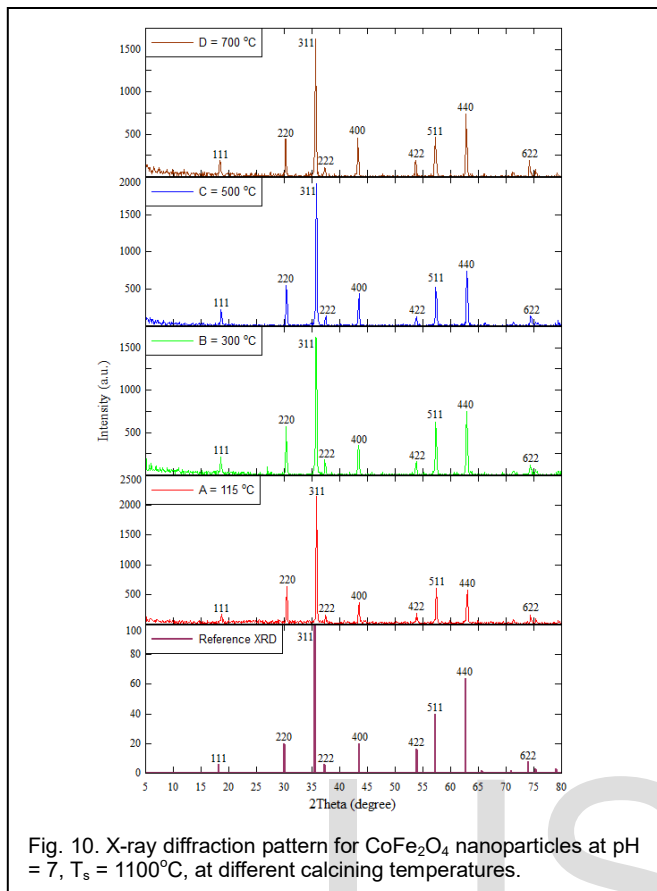


Fig. 10. X-ray diffraction pattern for  $\text{CoFe}_2\text{O}_4$  nanoparticles at  $\text{pH} = 7$ ,  $T_s = 1100^\circ\text{C}$ , at different calcining temperatures.

All samples exhibit similar diffraction peaks which correspond to the cubic spinel lattice of  $\text{CoFe}_2\text{O}_4$  (JCPDS Card No. 22-1086), from these diffraction patterns it is clear that many peaks with miller indices (h k l) are (111), (220), (311), (222), (400), (422), (511), (440) and (622), with  $2\theta = (18.288, 30.084, 35.437, 37.057, 43.058, 56.973, 75.009)$  all these peaks are indexed to the cubic spinel lattice, and the strongest peak was observed on (311) plane. The sharp diffraction peaks in above patterns indicate the appearance of the nano-crystals. Further the XRD patterns consist of fairly broad but still resolved peaks which were superimposed on slightly various intensity. Moreover, the peaks broadening points to the very small crystallite size and predict to nano-structured character of prepared material [4, 5, and 13]. Also we can see from these patterns, that the intensities of the strongest peak (311) increase with increasing the calcining temperatures of the powder that was prepared at temperature ( $115^\circ\text{C}$ ) and reach the maximum value at calcining temperature ( $700^\circ\text{C}$ ), this work agrees with powders with  $\text{pH}$  (3,7) and different the powder with  $\text{pH}$  (5), that indicates the crystallinity of the sample is improved.

Also from the (XRD) patterns we note that it is clear that peaks become sharper with the increasing in sintering temperature. This suggests that as the sintering temperature increases the crystallite size also increasing, because the sintering process generally decreases lattice defects and shrinkage,

but this technique can cause the coalescence of smaller grains, resulting in an increased average grain size for the nanoparticles. Finally, we show that the reflection planes of all samples which confirm on the presence of cobalt ferrite with a face-centered cubic structure. Also the results show that, as the calcination temperature increases, the diffraction peaks become sharper and narrower, and their intensity increasing. This indicates intensification in crystallinity that originates from the increment of crystalline volume ratio due to the particle size enlargement of the nuclei [14-17].

The crystallite size ( $D$ ) was determined by using the Scherrer's formula of the (311) plane of the prepared powder with different  $\text{pH}$ , calcined and sintered at different temperatures, also the X-ray density ( $\rho_x$ ) and lattice constant ( $a$ ) of these samples for the same peak and for different  $\text{pH}$  were calculated by using the equations (1,2 and 3 respectively) and as listed in Table (1, 2, 3), since this crystallographic plane exhibits the maximum diffraction intensity, these values of lattice constant ( $a$ ) are close to the bulk of  $\text{CoFe}_2\text{O}_4$  (8.395) [2,4, 18].

TABLE 1

pH	T(°C)	D(nm)	a(nm)	$\rho_x$ ( gm /cm <sup>3</sup> )
3	115	33	8.30	5.4
	300	42	8.26	5.5
	500	45	8.31	5.4
	700	59	8.36	5.3
5	115	48	8.28	5.4
	300	47	8.39	5.4
	500	50	8.35	5.3
	700	52	8.28	5.4
7	115	47	8.32	5.4
	300	46	8.32	5.4
	500	50	8.35	5.3
	700	51	8.35	5.3

Values of crystallite size ( $D$ ), the lattice constant ( $a$ ) and X-ray density ( $\rho_x$ ) of prepared powder of cobalt ferrite ( $\text{CoFe}_2\text{O}_4$ ) which calcined at different temperatures, for plane (311) for different  $\text{pH}$ .

Table (1) showed that the crystallite size ( $D$ ) and the lattice constant ( $a$ ) increased as the temperature increased, while X-ray density ( $\rho_x$ ) decreases when the temperatures increasing, this work is compatible with samples with  $\text{pH}$  (3,7), but this behavior is different at  $\text{pH}$  (5), that occurs due to particle sizes decrease when the temperatures increasing that is the temperature affects only the radius of the nanoparticles [19].



TABLE 2

pH	T(°C)	D(nm)	a(nm)	$\rho_x$ ( gm /cm <sup>3</sup> )
3	115	65	8.31	5.4
	300	60	8.33	5.3
	500	63	8.31	5.4
	700	67	8.31	4.1
5	115	67	8.33	5.3
	300	71	8.30	5.4
	500	77	8.33	5.3
	700	54	8.32	5.4
7	115	70	8.30	5.4
	300	72	8.30	5.4
	500	63	8.29	5.4
	700	70	8.33	5.3

Values of crystallite size (D), the lattice constant (a) and X- ray density ( $\rho_x$ ) of powder of cobalt ferrite (CoFe<sub>2</sub>O<sub>4</sub>) prepared which, calcined at different temperatures, for plane (311) for different pH, Ts(1000) °C.

TABLE 3

pH	T(°C)	D(nm)	a(nm)	$\rho_x$ ( gm /cm <sup>3</sup> )
3	115	58	8.34	5.3
	300	64	8.34	5.3
	500	59	8.31	5.4
	700	69	8.35	5.3
5	115	55	8.29	5.4
	300	70	8.32	5.4
	500	64	8.34	5.3
	700	63	8.30	5.4
7	115	68	8.32	5.4
	300	60	8.32	5.4
	500	69	8.30	5.4
	700	59	8.31	5.4

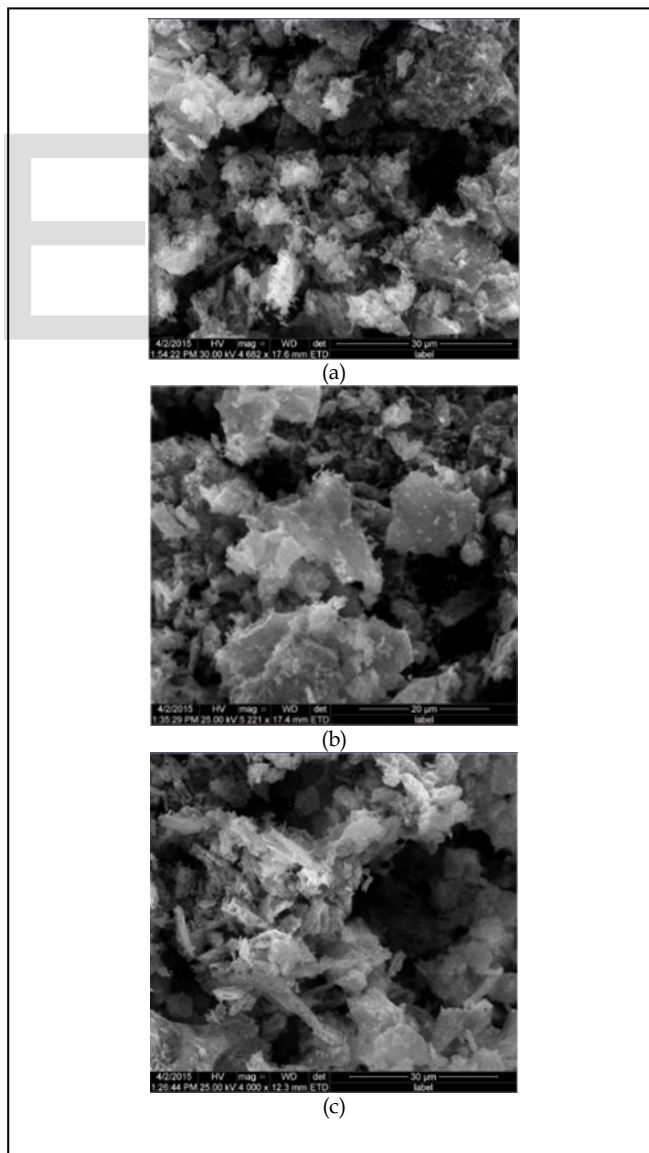
Values of crystallite size (D), the lattice constant (a) and X- ray density ( $\rho_x$ ) of prepared powder of cobalt ferrite (CoFe<sub>2</sub>O<sub>4</sub>), calcined at different temperatures, for plane (311) for different pH, Ts(1100) °C.

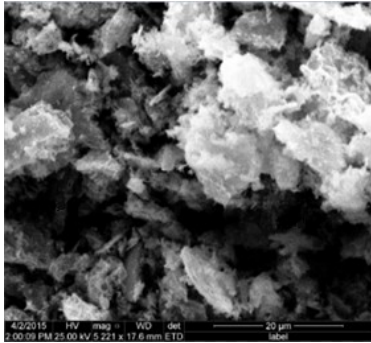
From above tables(1, 2) be observed that the crystallite size(D) and the lattice factor (a) increased as the calcining temperature increases, while X- ray density ( $\rho_x$ ) decreases when the calcining temperatures increasing, this explanation is compatible to samples with pH (3,7), but this behavior is different at pH (5), that occurs due to particles sizes decreases when the temperatures increasing that the temperature affects only the radius of the nanoparticles[19].while table (3) showed that the crystallite volume (D) and the lattice factor (a) increase the temperature increases, while X- ray density ( $\rho_x$ ) decreases when the temperatures increases, except the samples with pH (7) which show the crystallite size (D) and the lattice constant (a) decrease as the temperature increases, while X- ray density

( $\rho_x$ ) stay constant when the temperatures increases, because of particle sizes decreasing when the temperatures increasing, due to temperature affects only the radius of the nanoparticles[19].

#### 4.2 SEM

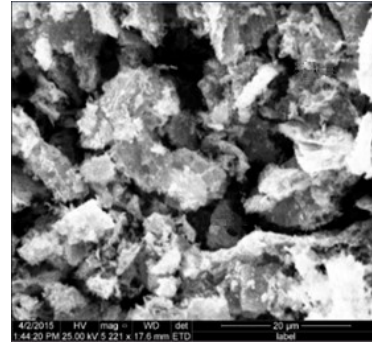
Figs (10, 11, and 12) shows the scanning electron micrographs of cobalt ferrite (CoFe<sub>2</sub>O<sub>4</sub>) nanoparticles powder, which was prepared by this method, with different pH, calcined at different temperatures. From these images we can observe, that the cobalt ferrite (CoFe<sub>2</sub>O<sub>4</sub>) nanoparticles powder has average sizes of nano-particles of about (119,111,99,97)nm of (pH=3) at calcined temperatures (300,500,700) °C respectively, and for( pH=5) the average sizes are (81,84,79,89)nm at calcined temperatures (300,500,700) °C respectively, finally for (pH=7) the average sizes are(77,50,34,23) nm at calcined temperatures (300,500,700) °C respectively. These values of the (SEM) results are in agreement with those calculated by Scherrer's equation and with (AFM) measurements.





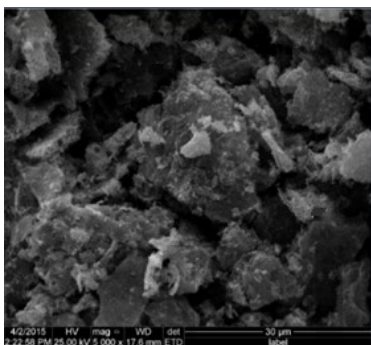
(d)

Fig. 10. Scanning electron micrograph of  $\text{CoFe}_2\text{O}_4$  nanoparticles, pH = 3, at different calcining temperatures.

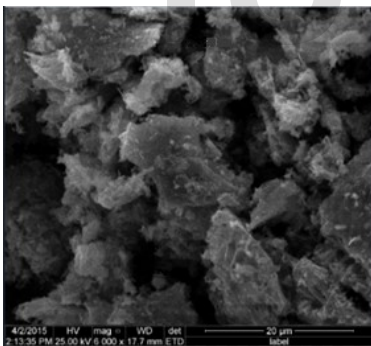


(d)

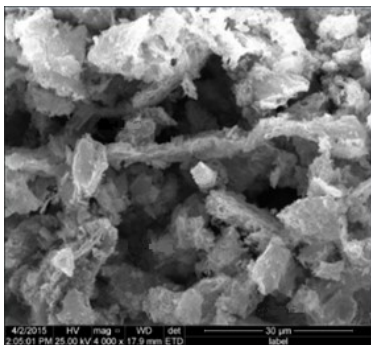
Fig. 11. Scanning electron micrograph of  $\text{CoFe}_2\text{O}_4$  nanoparticles, pH = 5, at different calcining temperatures.



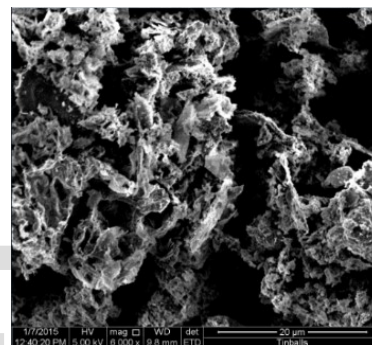
(a)



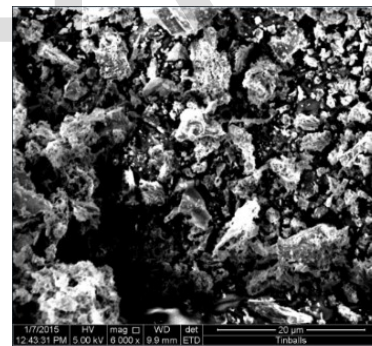
(b)



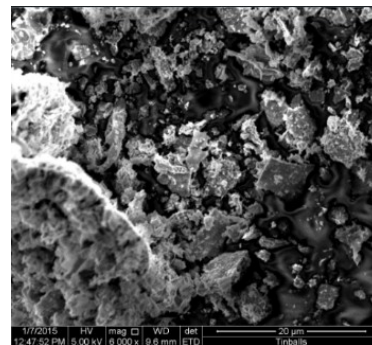
(c)



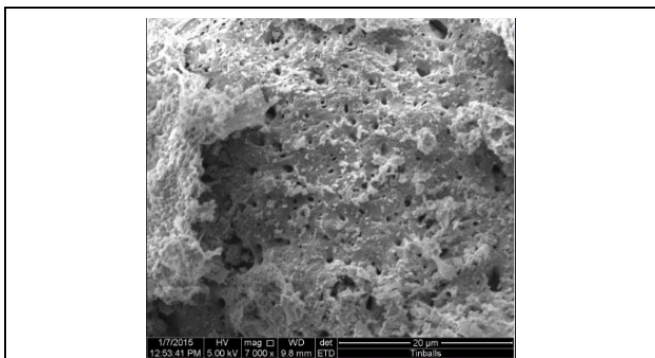
(a)



(b)



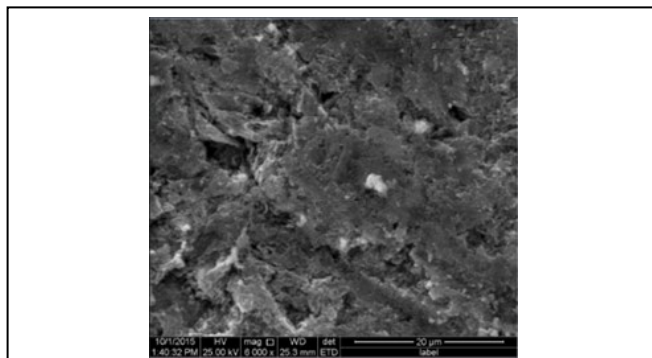
(c)



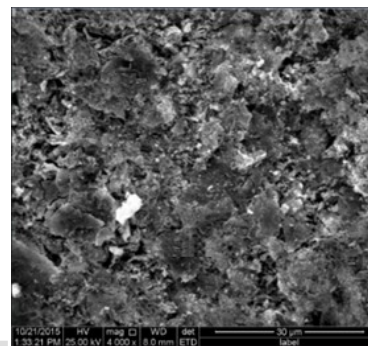
(d)

Fig. 12. Scanning electron micrograph of  $\text{CoFe}_2\text{O}_4$  nanoparticles, pH = 7, at different calcining temperatures.

Figs (13, 14, and 15) show the scanning electron microscope of samples which were made from cobalt ferrite ( $\text{CoFe}_2\text{O}_4$ ) nanoparticle powder, which was prepared by sol-gel auto-combustion method, with different pH, calcined at different temperatures and sintering temperature ( $1000$ ) °C. From these images we can observe, that the samples have average sizes of nano-particles of about (111,108, 97,96) nm of (pH=3) at calcined temperatures (300,500,700) °C respectively, and for (pH=5) the average sizes are (23,94,87,101) nm calcined temperatures (300,500,700) °C respectively, finally for (pH=7) the average sizes are (75,48,32,22) nm at calcined temperatures (300,500,700) °C respectively. These values of the (SEM) results are in agreement with those calculated by Scherrer's equation and with (AFM) measurements.

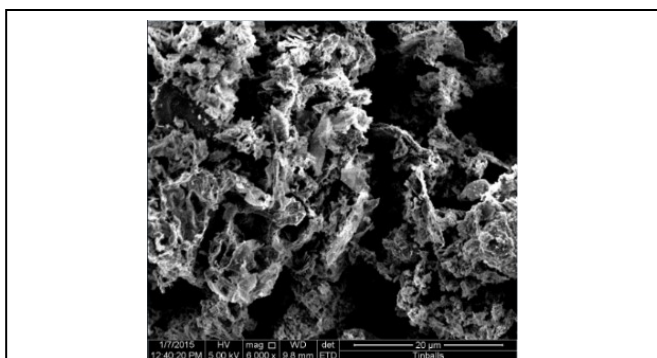


(c)

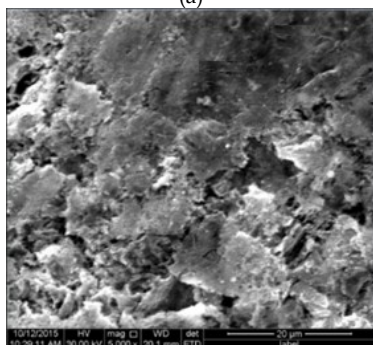


(d)

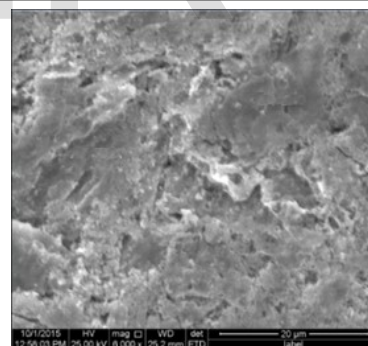
Fig. 13. Scanning electron micrograph of  $\text{CoFe}_2\text{O}_4$  nanoparticles, pH = 3,  $T_s = 1000^\circ\text{C}$ , at different calcining temperatures.



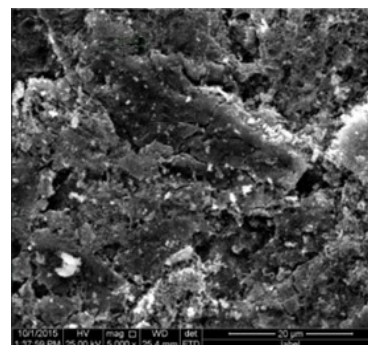
(a)



(b)

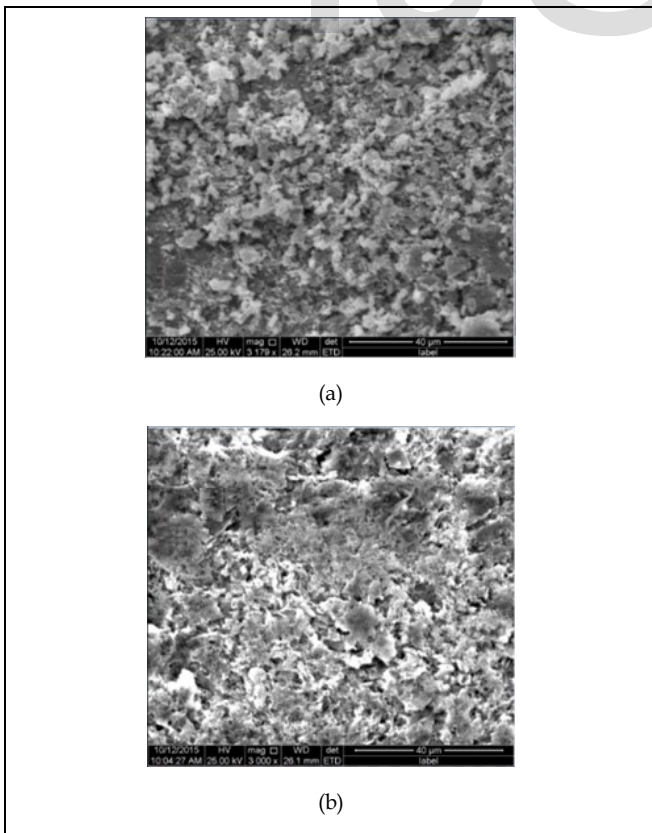
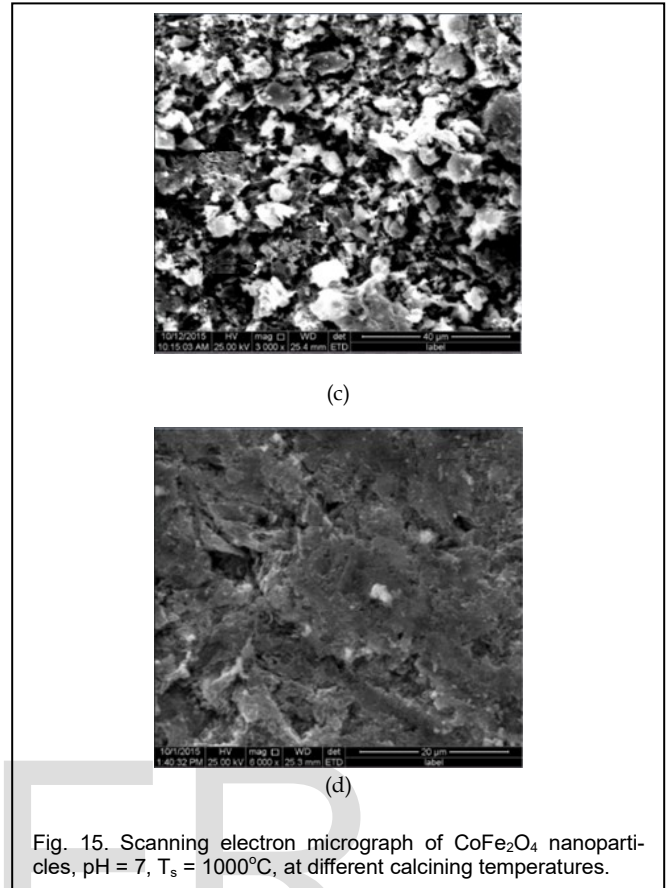
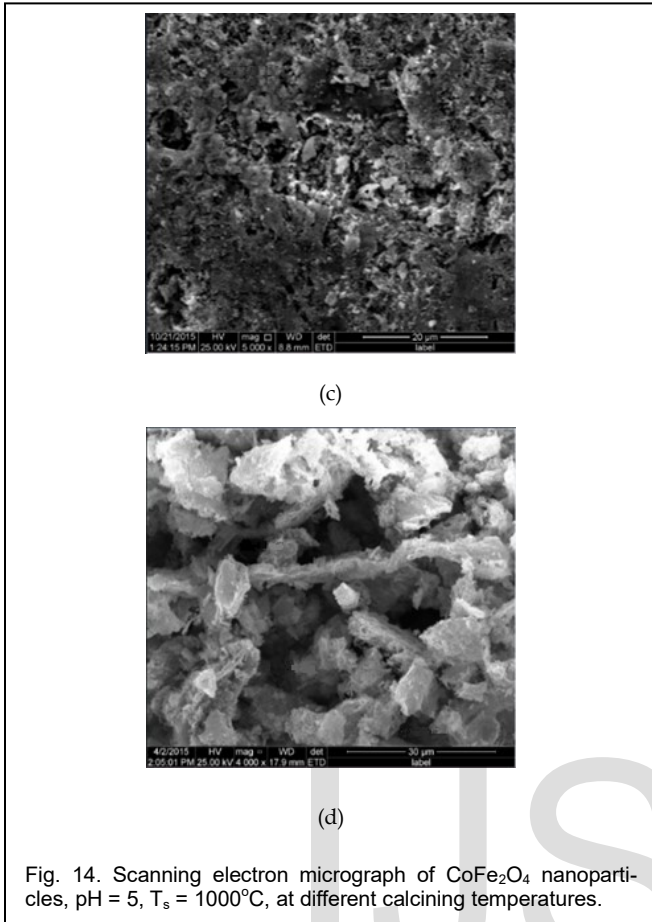


(a)

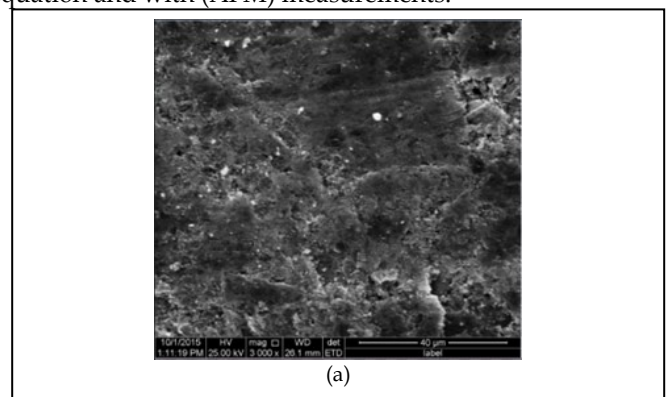


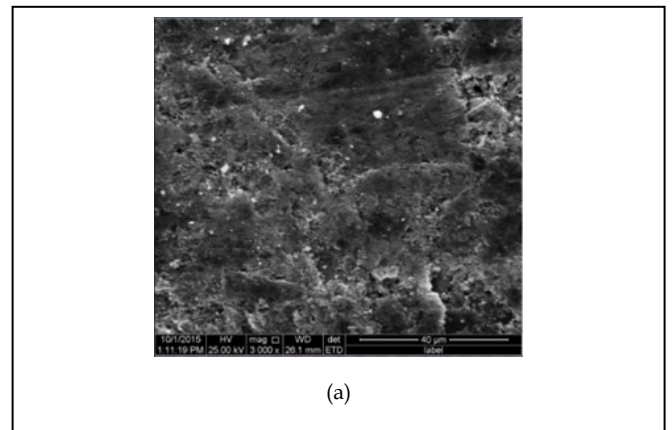
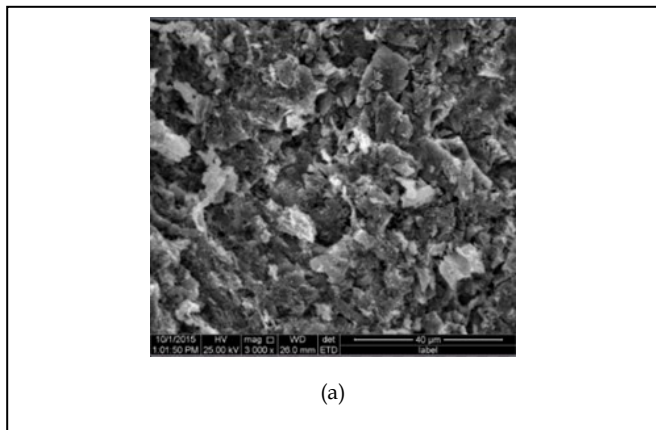
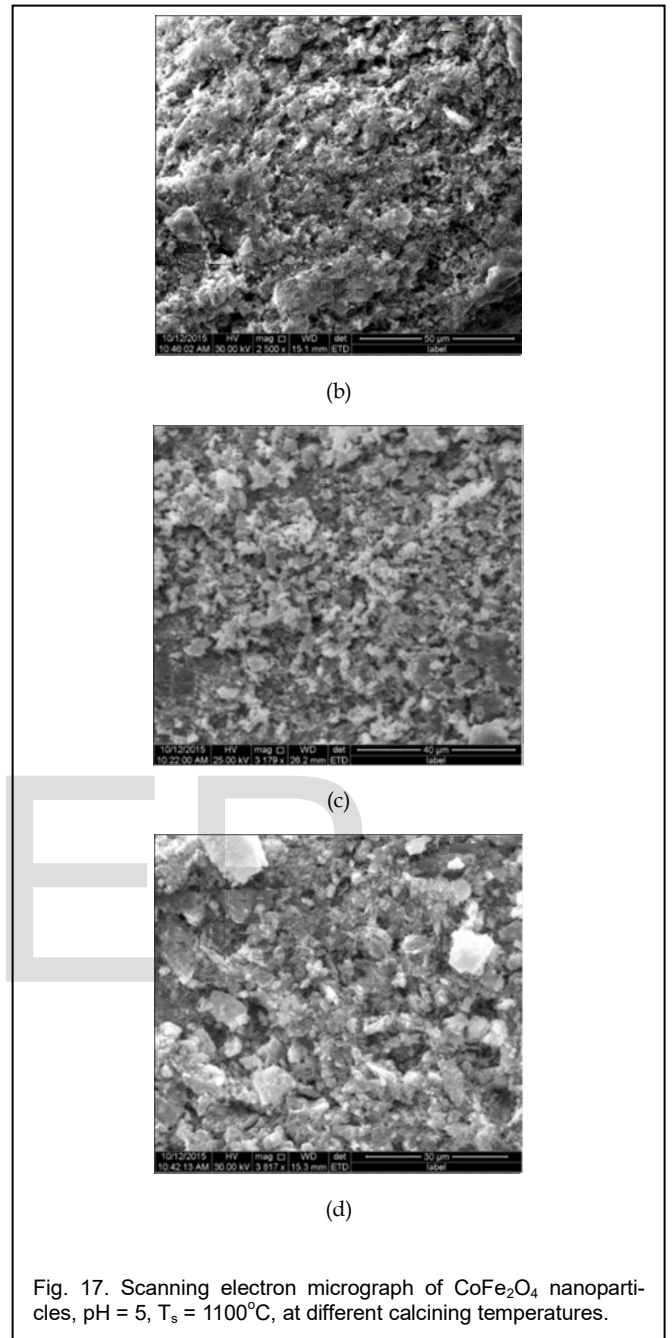
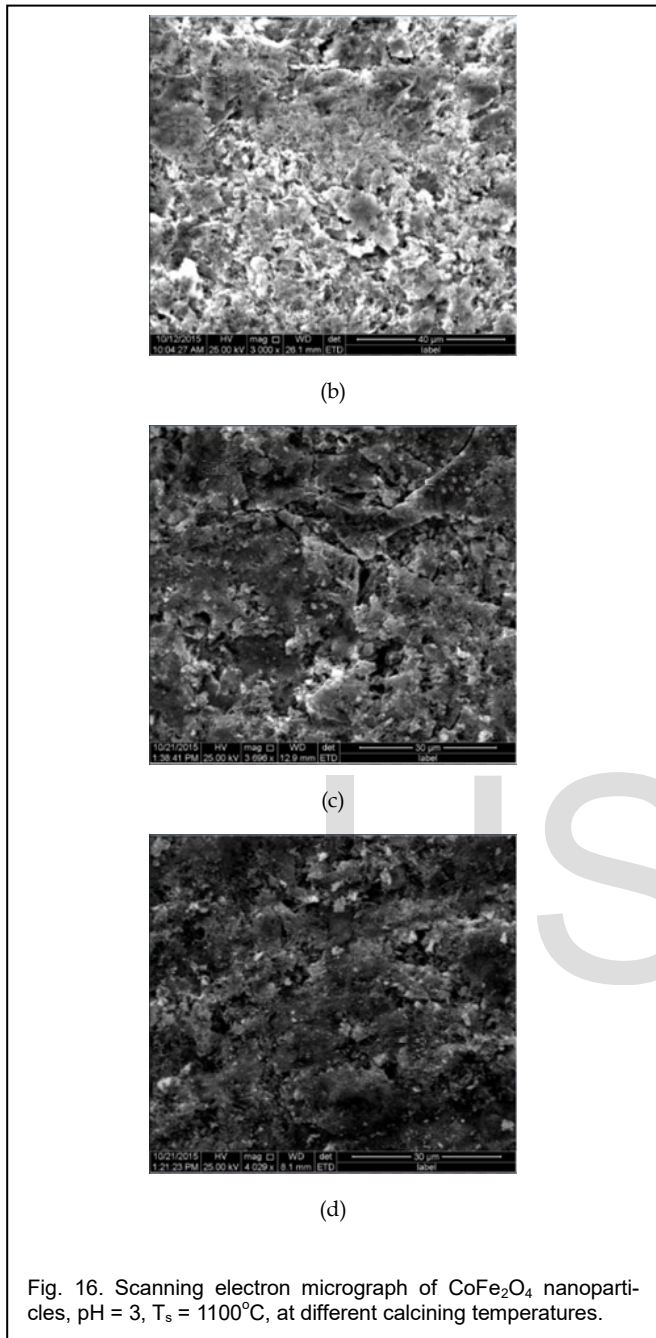
(b)





Figs (16, 17, 18) show the scanning electron microscope of samples which made from cobalt ferrite ( $\text{CoFe}_2\text{O}_4$ ) nanoparticles powder, prepared by sol-gel auto-combustion method, with different pH, calcined at different temperatures and sintered temperature at  $(1100)^\circ\text{C}$ . From these images we can observe, that the samples have average sizes of nanoparticles of about (98,95,125,80) nm of (pH=3) at calcined temperatures (115,300,500,700)  $^\circ\text{C}$  respectively, and for (pH=5) the average sizes are (102,102,108,119)nm calcined at temperatures (115,300,500,700)  $^\circ\text{C}$  respectively, finally for (pH=7) the average sizes are(119,70,45,36,20) nm at calcined temperatures (115,300,500,700)  $^\circ\text{C}$  respectively. These values of the (SEM) results are in agreement with those calculated by Scherrer's equation and with (AFM) measurements.







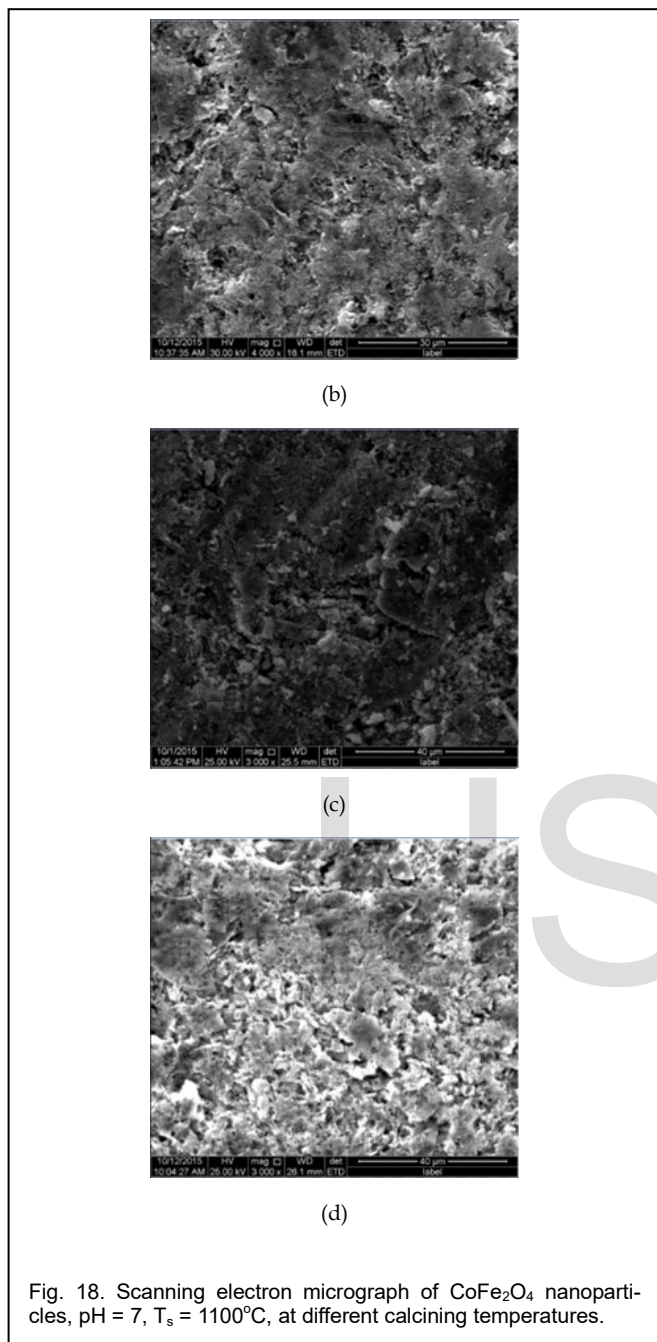


Fig. 18. Scanning electron micrograph of  $\text{CoFe}_2\text{O}_4$  nanoparticles, pH = 7,  $T_s = 1100^\circ\text{C}$ , at different calcining temperatures.

The products contained spherical particles but to some extent aggregations were observed in each sample.  $\text{CoFe}_2\text{O}_4$  nanoparticles prepared in this method have uniform, mono-dispersive spherical structure with a narrow size distribution of particles, coral like structural morphology, features indicative of nano crystalline nature, with pores, the porous feature of agglomerate is attributed to the liberation of a large amount of gas during the combustion, and also we observed that there is agglomeration among the particles, which are associated to the magnetization of ferrite. The (SEM) images show that the average particles size decreases when the calcining temperatures increase, this occurs due to the temperature that affects only the radius of the nanoparticles, ex-

cept the samples with (pH=5) [4,5,20].

We also observed from all figures that the the sample without calcining process has a loosely bound powderly mass with lot of voids visible, while when we are calcined samples, there is a change into more cohesive, dense and crystalline compound, and when we increase the calcining temperature lead that to form uniform compound with a definite crystalline structure evident from the material and also are showed a highly dense, uniform size and is distributed cobalt ferrite ( $\text{CoFe}_2\text{O}_4$ ) with well defined grain boundary. The cubic lattice of the spinel and continuous bonding between groups are clearly visible at higher magnification. Also we observed that when the sintering temperature increasing the average grain size decreasing except the samples with pH(5).

#### 4.3 EDS Test

The Energy Dispersive Spectroscopy (EDS) is used to confirm the ratio of the transition metal atom in each material according to the nominal stoichiometry, and is used to determine nanoparticles.

The spectrum of cobalt ferrite ( $\text{CoFe}_2\text{O}_4$ ) nanoparticles powder was prepared by this method, with different pH, calcined at different temperatures of is shown in Fig. (19). At the same time this figure is identical to the samples which were made from cobalt ferrite ( $\text{CoFe}_2\text{O}_4$ ) nanoparticle powder, prepared by using nanoparticles powder, which was prepared by the same method, with different pH, calcined at different temperatures and sintered at different temperatures.

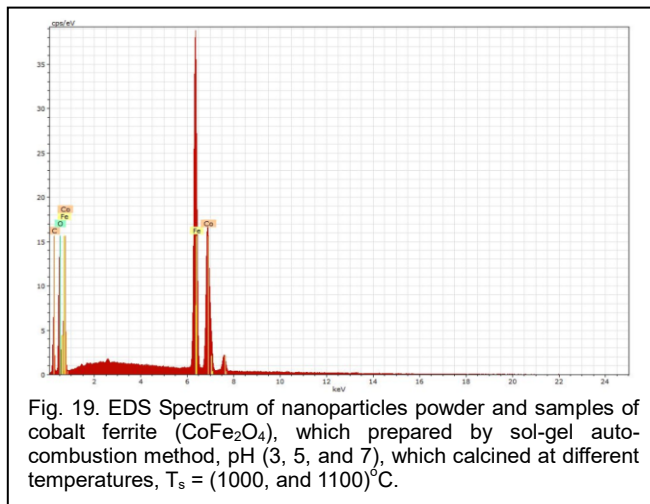


Fig. 19. EDS Spectrum of nanoparticles powder and samples of cobalt ferrite ( $\text{CoFe}_2\text{O}_4$ ), which prepared by sol-gel auto-combustion method, pH (3, 5, and 7), which calcined at different temperatures,  $T_s = (1000, \text{ and } 1100)^\circ\text{C}$ .

From this figure it is clear that Co: Fe ratio is 1:2 indicates that the stoichiometric proportion is used that leads to prove the Co: Fe ratio maintains entire calcined sample. These results revealed the sustained spinel structure of the  $\text{CoFe}_2\text{O}_4$  crystal at low calcinations temperature. As can be seen, the prepared material contains cobalt, iron, and oxygen, carbon are present in prepared material as common organic pollution [21].

Also Table (4) shows the composition of nanoparticles powder and samples of cobalt ferrite ( $\text{CoFe}_2\text{O}_4$ ), which prepared by this method, with different pH, calcined and sintered at different temperatures observed by the EDS spectrum. These results revealed the sustained spinel structure of cobalt ferrite ( $\text{CoFe}_2\text{O}_4$ ) nanoparticles powder, is prepared by this method [4, 19].

TABLE 4

El	AN	Series	unn. c	norm. c	Atom. c	Error (1Sigma)
			[wt.%]	[wt.%]	[at.%]	[wt.%]
C	6	K-series	55.48	47.01	69.31	8.63
Fe	26	K-series	26.23	22.23	7.05	0.70
O	8	K-series	21.07	17.85	19.76	2.96
Co	27	K-series	15.25	12.92	3.88	0.42
Total			118.03	100.00	100.00	

Composition of nanoparticles powder and samples of cobalt ferrite ( $\text{CoFe}_2\text{O}_4$ ), which was prepared by sol-gel auto-combustion method, pH(3,5,7), which was calcined at different temperatures,  $T_s(1000,1100)^\circ\text{C}$  obtained by the EDS spectrum.

#### 4.4 AFM Test

The particle size, surface roughness average and the surface morphology of the prepared material were determined by using Atomic Force Microscope (AFM). The (AFM) images of surface morphology for the cobalt ferrite ( $\text{CoFe}_2\text{O}_4$ ) nanoparticles powder, prepared by this method with different pH, at different calcining, sintering temperatures are shown in Figs (20, 21, 22, 23, 24, 25, 26, 27, 28) respectively:

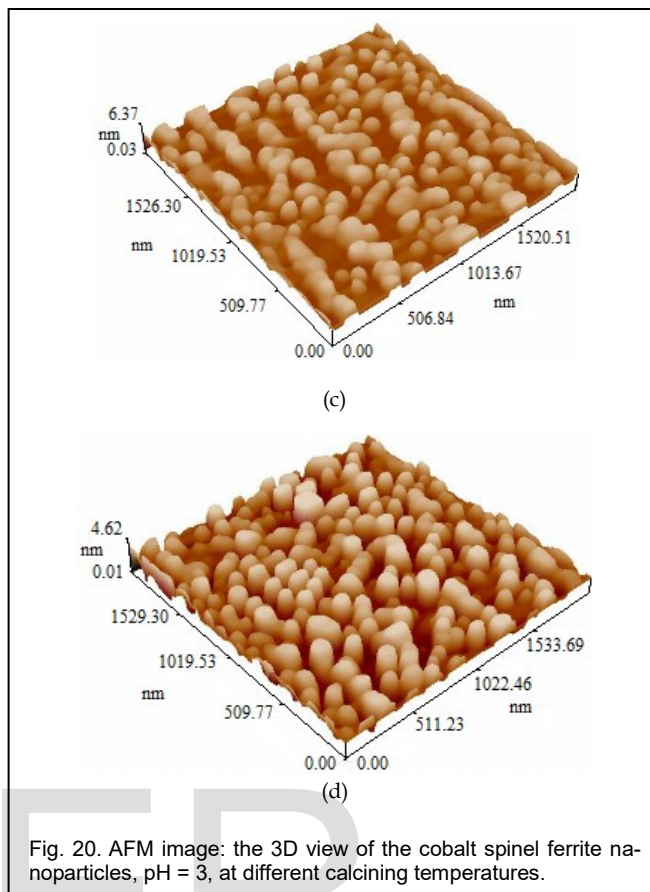
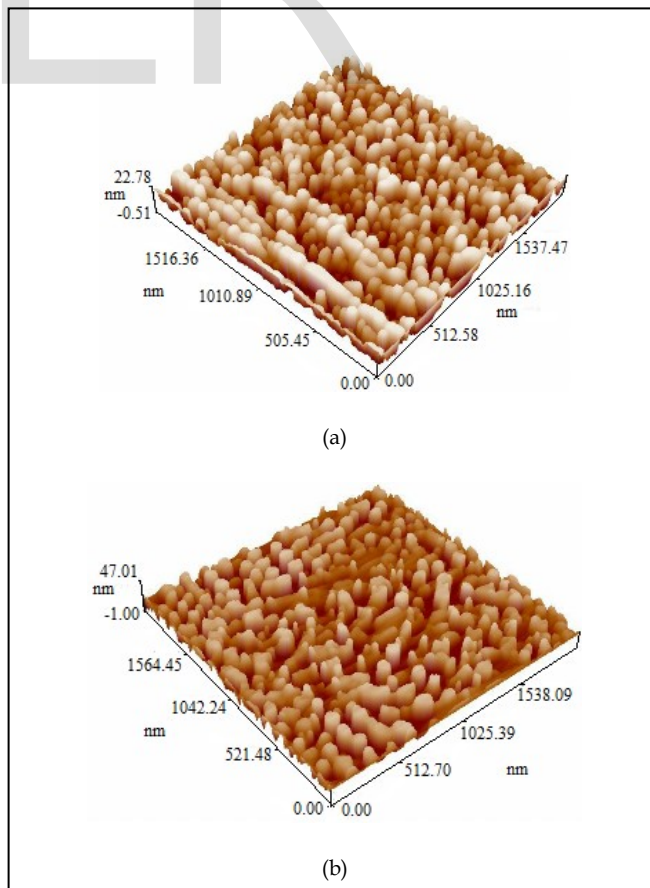
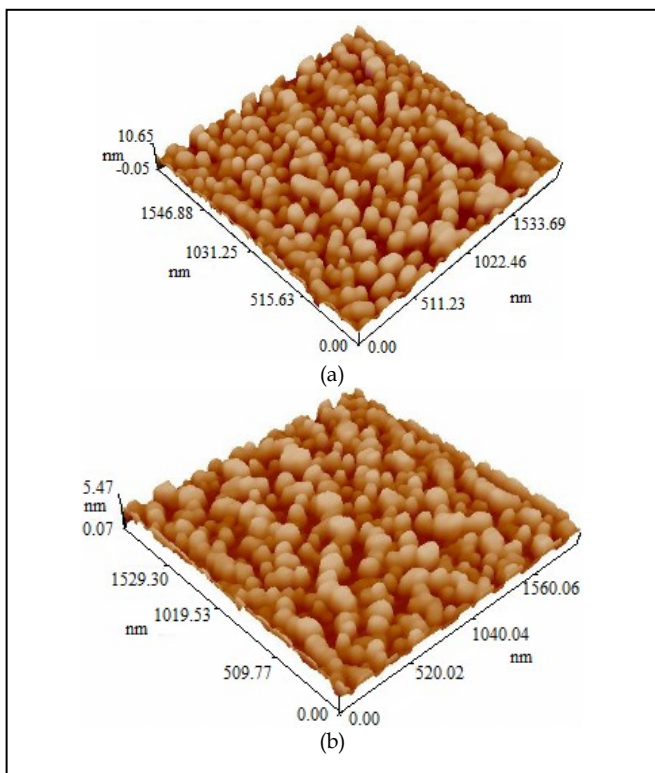


Fig. 20. AFM image: the 3D view of the cobalt spinel ferrite nanoparticles, pH = 3, at different calcining temperatures.





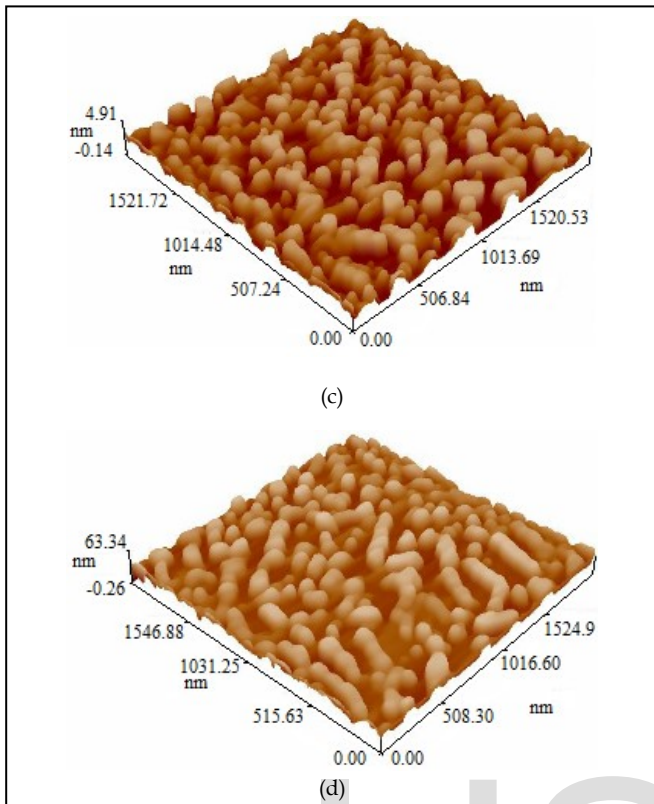


Fig. 21. AFM image: the 3D view of the cobalt spinel ferrite nanoparticles, pH = 5, at different calcining temperatures.

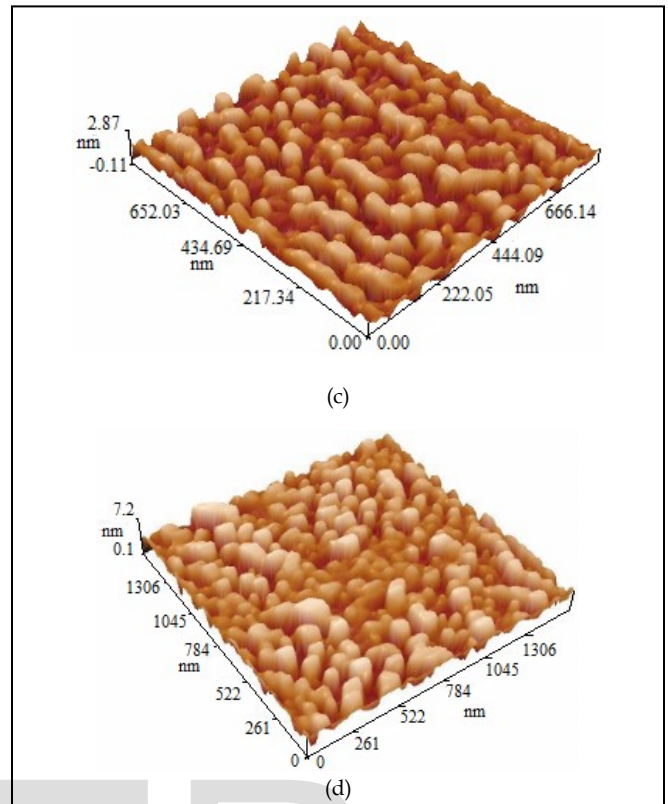
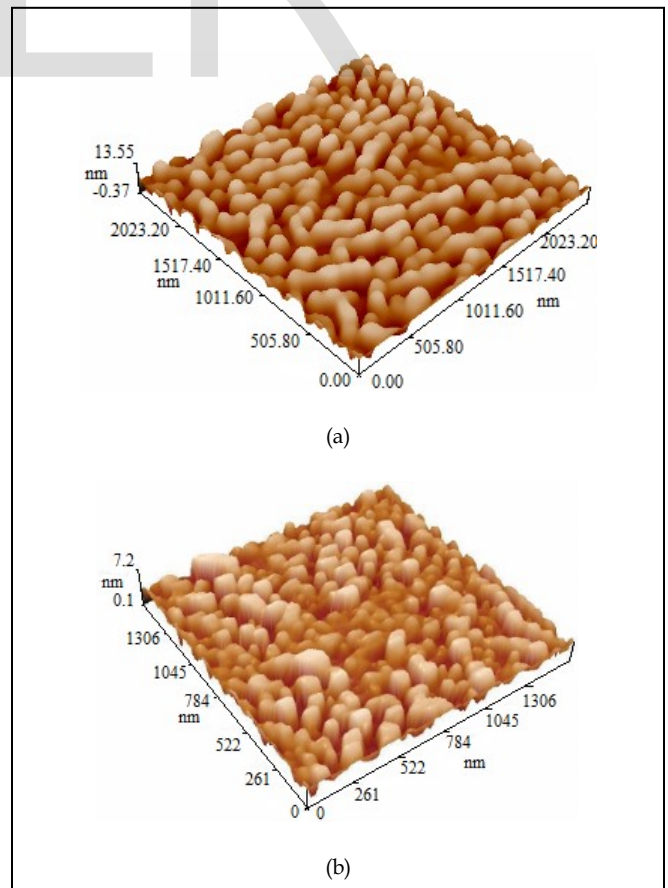
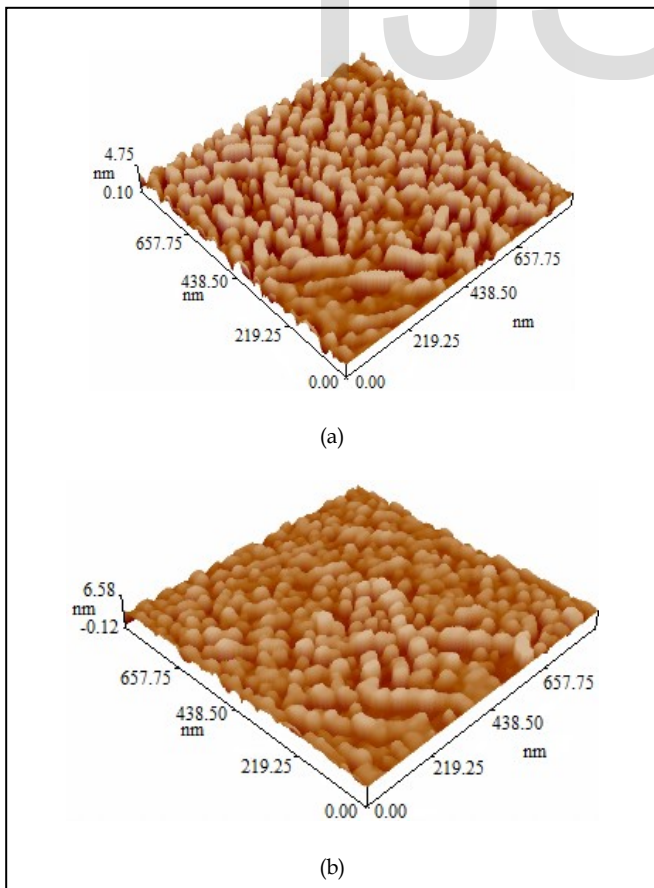
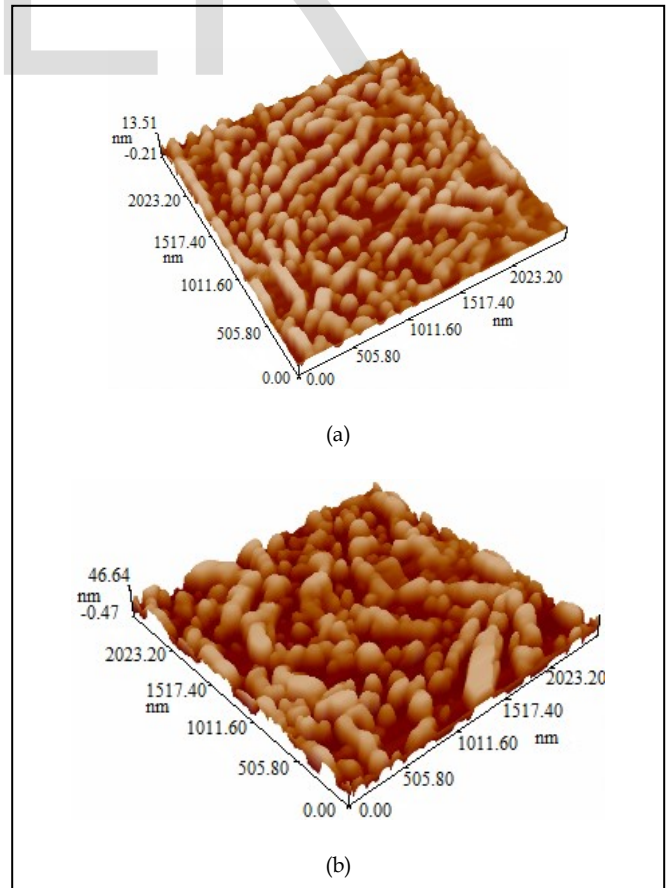
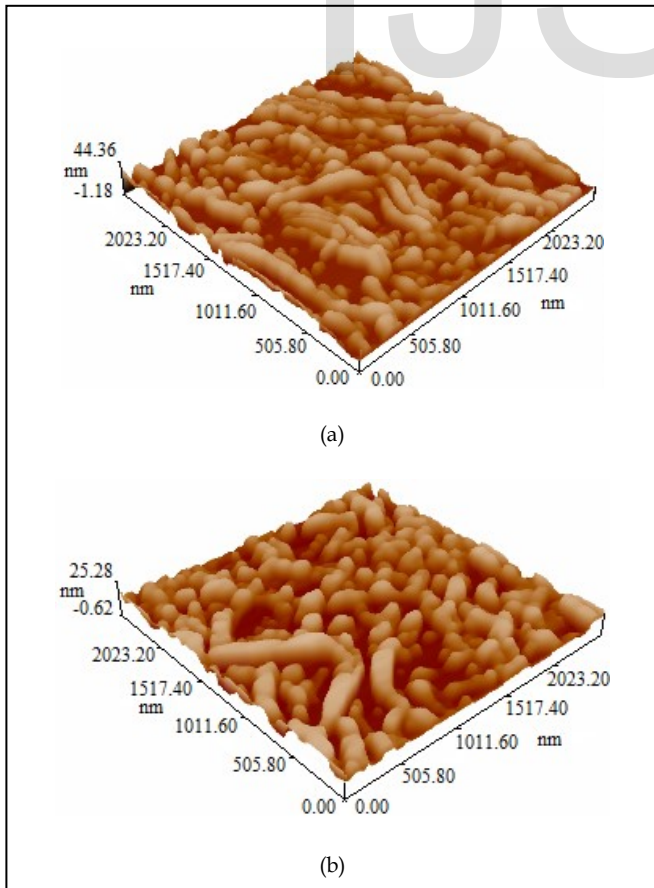
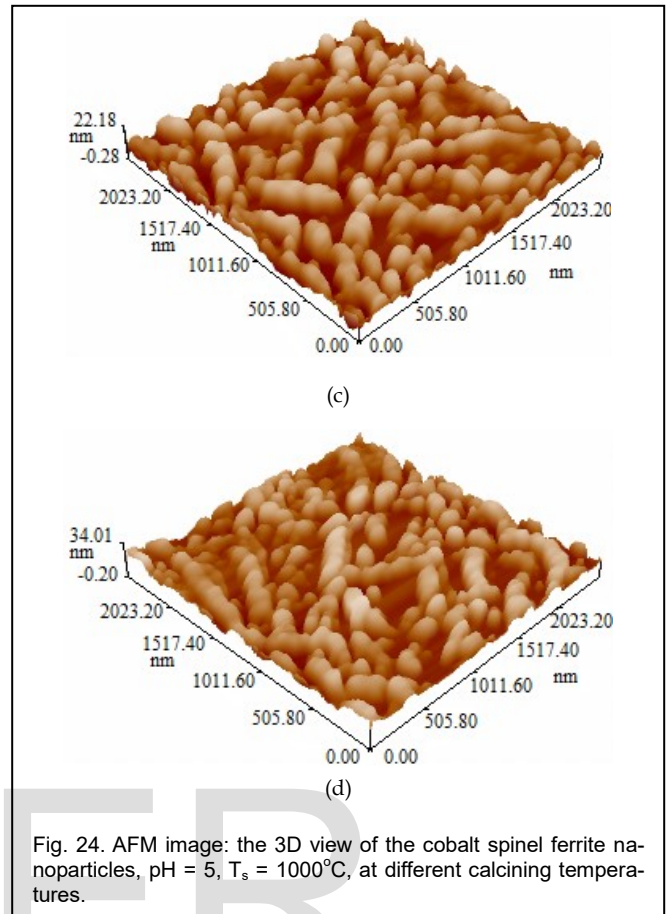
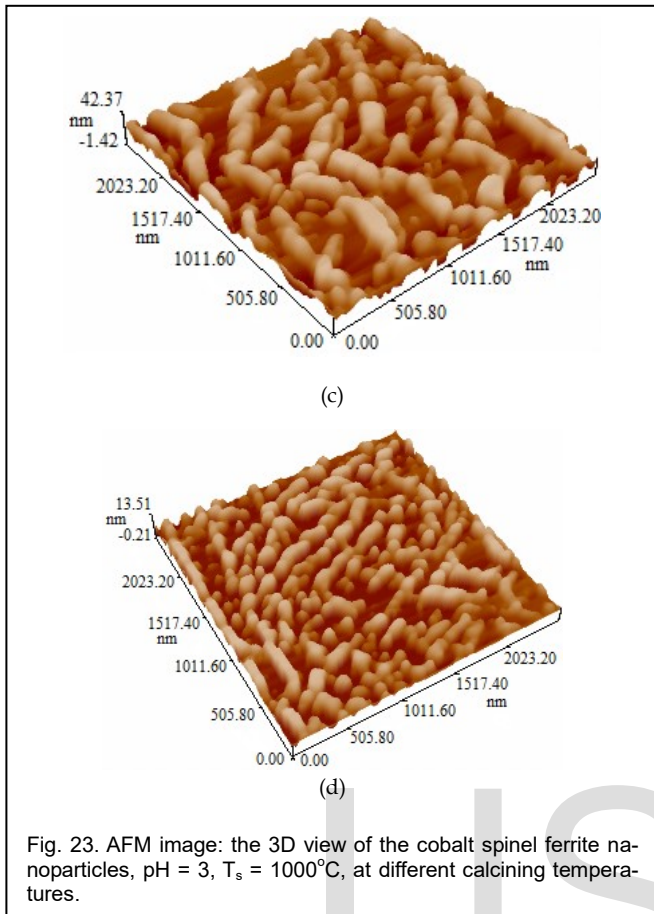
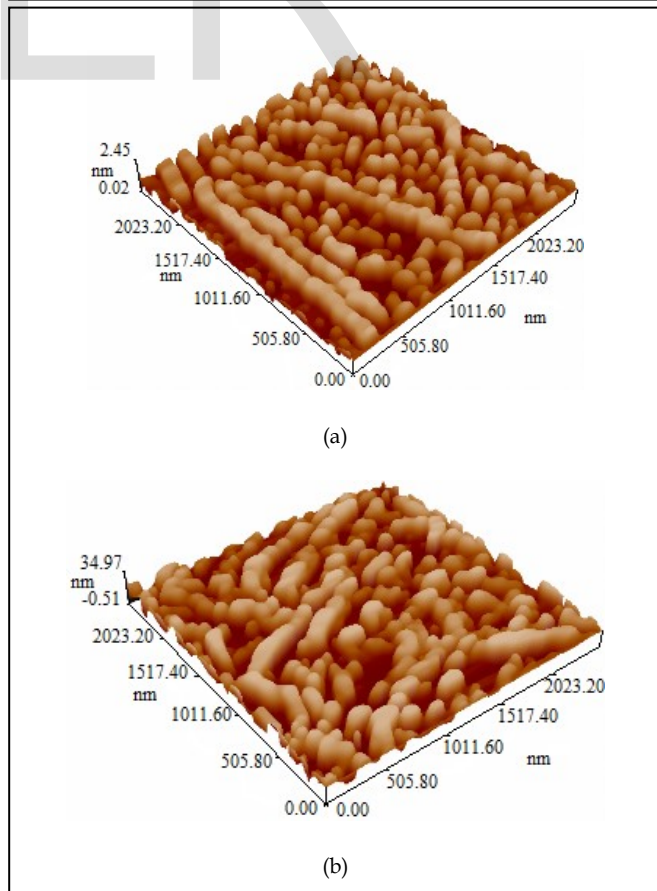
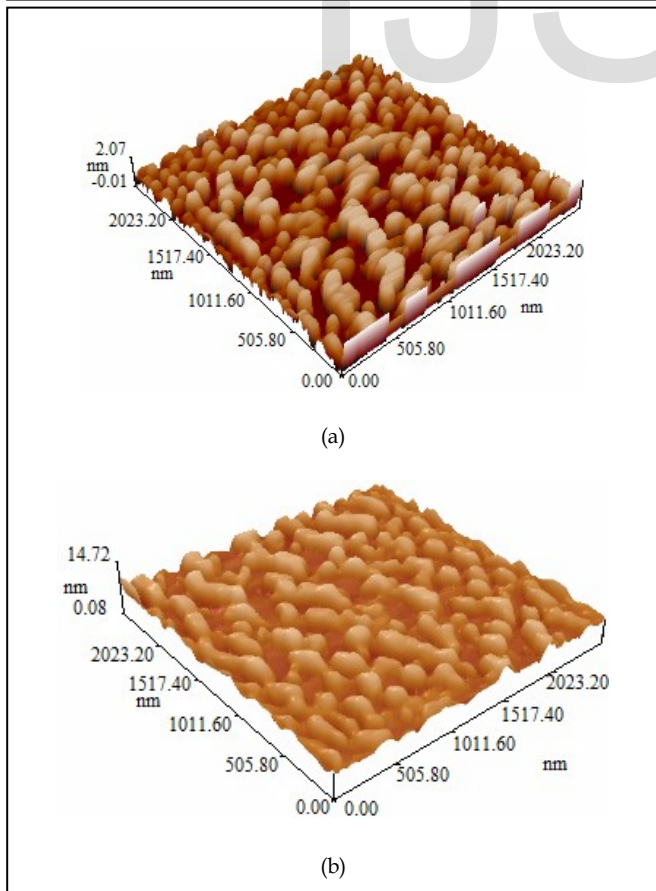
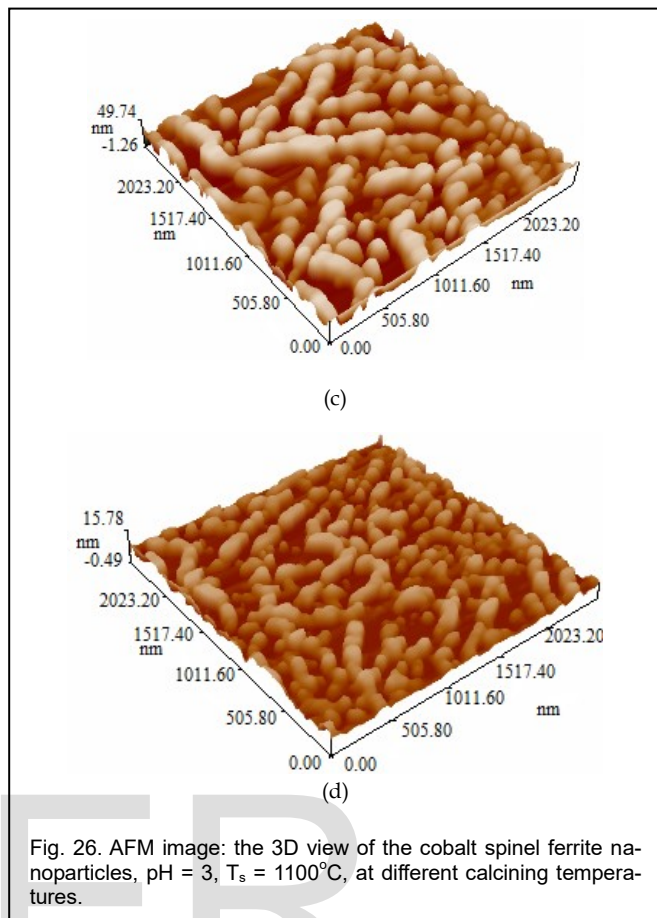
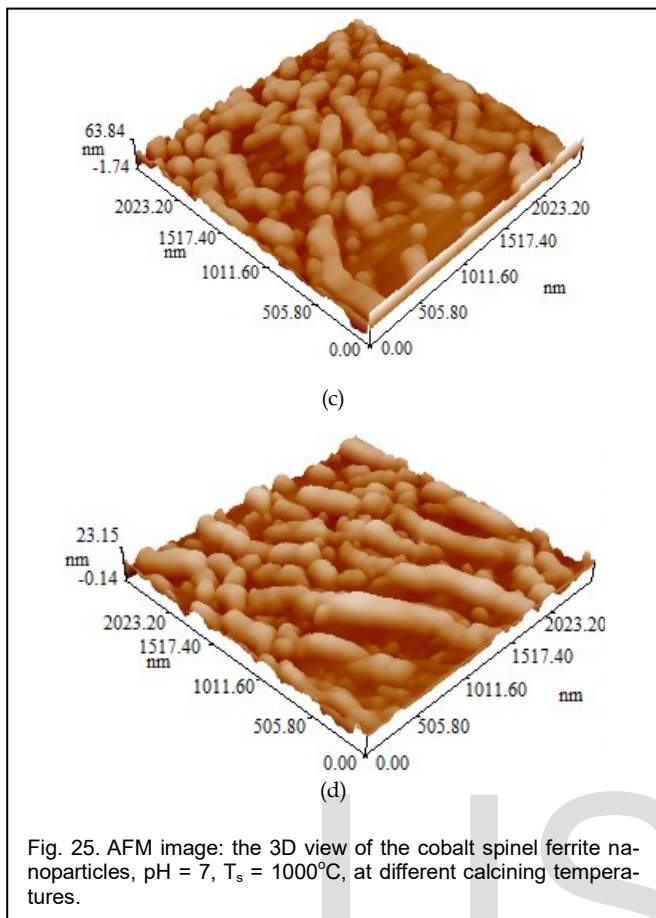


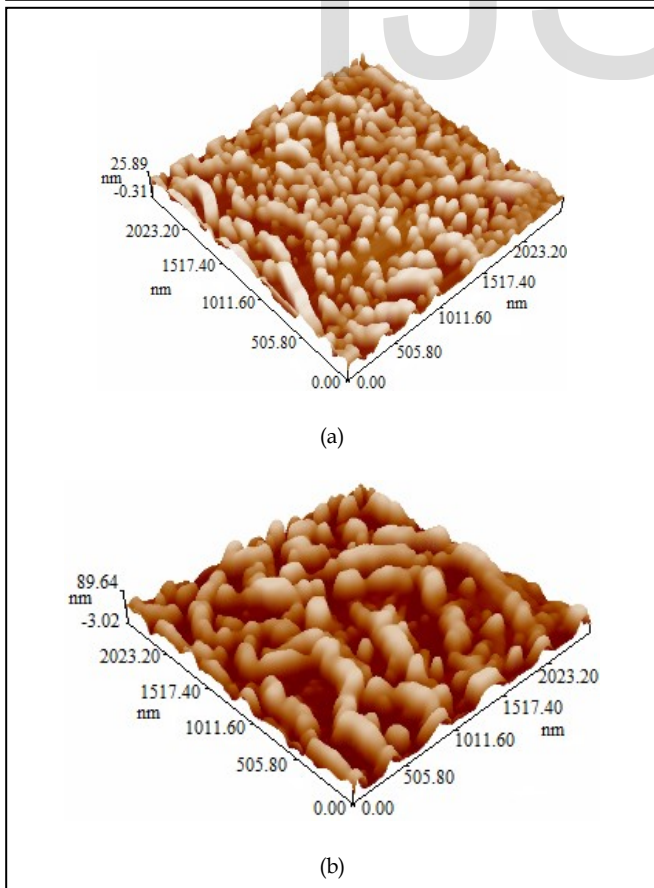
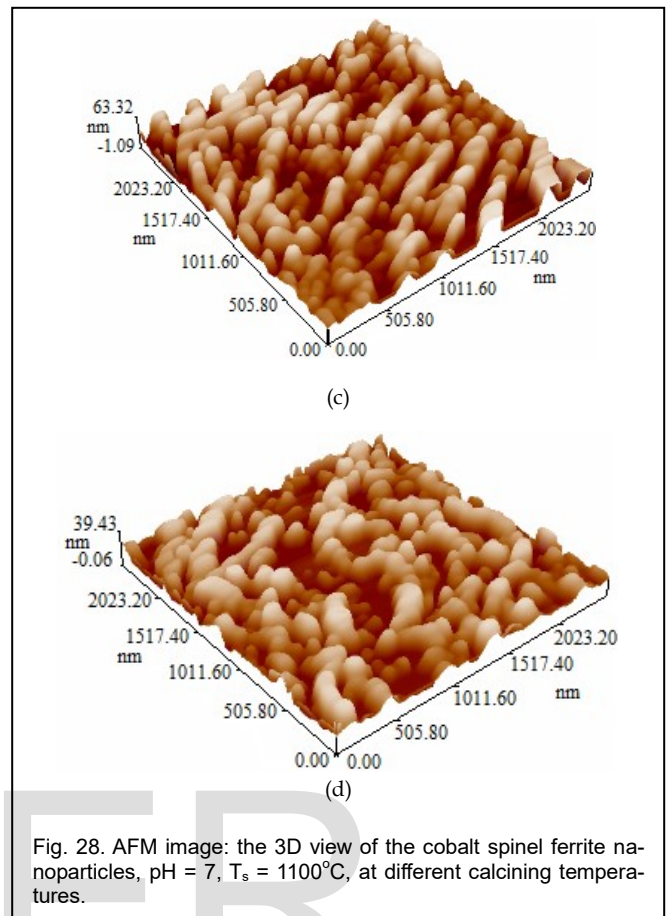
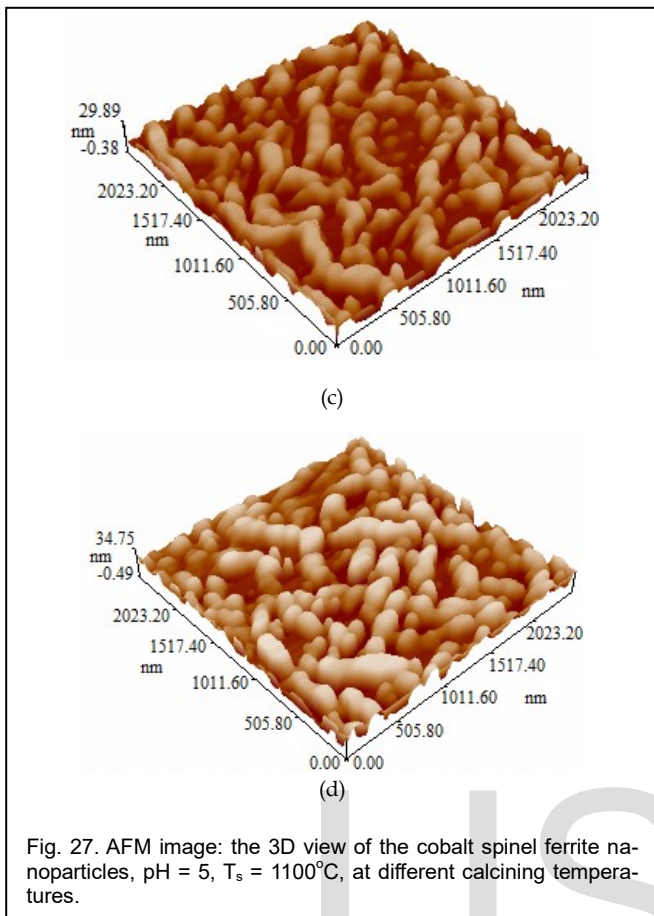
Fig. 22. AFM image: the 3D view of the cobalt spinel ferrite nanoparticles, pH = 7, at different calcining temperatures.











In these images it is clear that a uniform structure without any valleys is observed and all the particles are aligned vertically due to the homogeneously distribution of the ferrite particles [9, 22].

The averages diameter of particle size, roughness averages of cobalt ferrite ( $\text{CoFe}_2\text{O}_4$ ) nanoparticles powder, are shown in table (5, 6, 7).

TABLE 5

pH	Temperature ( $^\circ\text{C}$ )	Average diameter (nm)	Roughness average (nm)
3	115	119.55	1.6
	300	111.87	0.74
	500	99.08	0.74
	700	97.31	0.88
5	115	81.53	5.14
	300	84.04	12.3
	500	79.16	0.73
	700	89.94	7.24
7	115	77.31	1.04
	300	50.86	0.953
	500	34.58	0.82
	700	23.53	0.489

Effect of calcining temperature and pH on, the averages diameter of particle size, roughness averages prepared with different pH, at different calcining temperatures.



TABLE 6

pH	Temperature (°C)	Average diameter (nm)	Roughness average (nm)
3	115	111.80	8.4
	300	108.88	6.33
	500	97.18	2.38
	700	96.04	2.99
5	115	23.20	5.61
	300	94.76	3.59
	500	87.23	3.32
	700	101.47	4.62
7	115	75.80	1.27
	300	48.80	0.815
	500	32.50	0.719
	700	22.30	0.329

Effect of calcining temperature and pH on the average diameter of particle size, roughness averages of samples which were prepared from Cobalt Ferrite (CoFe<sub>2</sub>O<sub>4</sub>), with different pH at different calcining temperatures, Ts=1000 ° C.

TABLE 7

pH	Temperature (°C)	Average diameter (nm)	Roughness average (nm)
3	115	98.27	0.409
	300	95.67	1.33
	500	125.43	8.96
	700	80.79	1.97
5	115	102.51	0.415
	300	102.96	4.26
	500	108.89	6.11
	700	119.68	6.26
7	115	70.22	1.19
	300	45.04	0.80
	500	36.90	0.39
	700	20.79	0.225

Effect of calcining temperature and pH on the averages diameter of particle size, roughness averages of samples which prepared from Cobalt Ferrite (CoFe<sub>2</sub>O<sub>4</sub>), with different pH at different calcining temperatures, Ts=1100 ° C.

From these tables it be observed that the averages diameter of particle size, roughness average of samples prepared from Cobalt Ferrite (CoFe<sub>2</sub>O<sub>4</sub>) with different pH, at different calcining temperatures, at different sintering temperatures, decreases when the temperatures increases.

That occurs due to particle size decreases when the temperatures increase, the temperature affects only the radius of the nanoparticles, this behavior agrees with samples with pH (3,7) and discrepancy on samples with pH (5) and the good values we obtained of samples with pH (7), at sintering

temperature (1100)°C.

It can also be observed that the samples sintered at temperature (1100) ° C have the values of average diameter of particle size and roughness average lower than these samples without sintering, and the samples sintered at (1000) ° C, that occurs due to particles size decreases when the temperature increasing, this occurs because the temperature affects only the radius of nanoparticles [19].

## 5 CONCLUSION

In this work Cobalt ferrite nanoparticles powder have been successfully synthesized at a sufficiently low temperature by sol- gel auto combustion technique. The crystallite volume (*D*) and the lattice factor (*a*) rise as the temperature rise, while X-ray density (*ρ<sub>x</sub>*) decreases when the temperatures increase, this word is compatible on samples with pH (3,7), but this behavior is different at pH (5). As the sintering temperature increases the crystallite size also increases, due to the sintering process generally decreases lattice defects and shrinkage, but this technique can cause the coalescence of smaller grains, resulting in an increased average grain size for the nanoparticles. The (SEM) results are agreed with those calculated by Scherrer's equation and with (AFM) measurements. It is clear that Co: Fe ratio is 1:2 indicating that the stoichiometric proportion is used, which lead to prove the Co: Fe ratio is maintained. Finally, the images of (AFM) showed that a uniform structure without any valleys was observed and all the particles are aliened vertically due to the homogenously distribution of the ferrite particles.

## REFERENCES

- [1] Venkata Kumar Vagolu, K. Samatha, K. Chandra mouli, J. N. Kiran and Paul douglas Nasi, "Preparation and characterization of polycrystalline mixed Nickel Zinc Ferrites for dielectric properties and practical application," *Int. J. of Pharma & Bio Sciences*, Vol.5, No. 3, pp. 159 – 175, 2014.
- [2] Hemaunt Kumar, R. C. Srivastava, P. Negi, H. M. Agrawal and K. Asokandieletric, "Dielectric behaviour of cobalt ferrite nanoparticles," *Int. J. E. & E. (IJEEE)*, ISSN 2278-9944, Vol. 2, Issue 1, pp. 59-66, 2013.
- [3] Leena Jaswala and Brijesh Singhb, "Ferrite materials: a chronological

- review," *J. Integr. Sci. Technol.*, Vol.2, No.2, pp. 69-71, 2014.
- [4] Saeed Abedini Khorrami, and Qazale Sadr Manuchehri, "Magnetic properties of cobalt ferrite synthesized by hydrothermal and Coprecipitation methods: a comparative study," *Journal of Applied Chemical Research*, Vol. 7, No.3, pp. 15-23, 2013.
- [5] Raghavender AT, "Synthesis and characterization of cobalt ferrite nanoparticles," *STAR Journal*, Vol.2, No.4, pp. 1-4, 2013.
- [6] Zuzana Kozakova, Ivo Kuritka, Pavel Bazant, Michal Machovsky, Miroslav Pastorek, and Vladimir Babayna, "Simple and effective preparation of cobalt ferrite nanoparticles by microwave-assisted solvo thermal Method," *Brno, Czech Republic, EU*, Vol.10, pp.23- 25, 2012.
- [7] A.B. Shinde, "Structural and electrical properties of cobalt ferrite nanoparticles," *International Journal of Innovative Technology and Exploring Engineering (IJITEE)*, ISSN: 2278-3075, Vol. 3, Issue 4, pp. 64-67, 2013.
- [8] Zhenfa Zi, Yuping Sun, Xuebin Zhu, Zhaorong Yang, Jianming Dai, and Wenhai Song, "Synthesis and magnetic properties of  $\text{CoFe}_2\text{O}_4$  ferrite nanoparticles," *J. of M. & M. M.*, Vol.321, pp. 1251-1255, 2009.
- [9] P. vlazana, and M. vassle, "Synthesis and characterization  $\text{CoFe}_2\text{O}_4$  nanoparticles prepared by the hydrothermal method," *optoelectronics and advanced materials – rapid communications*, Vol. 4, No. 9, pp. 1307 – 1309, 2010.
- [10] M. Sajjia, M. Oubaha, T. Prescott, and A.G. Olabi, "Development of cobalt ferrite powder preparation employing the sol-gel technique and its structural characterization," *EPJ Web of conferences*, Vol. 6, pp. 05003, 2010.
- [11] S. S. Madani, G. Mahmoudzadeh, and S. Abedini Khorrami, "Influence of pH on the characteristics of cobalt ferrite powder prepared by a combination of sol-gel auto-combustion and ultrasonic irradiation techniques," *Journal of Ceramic Processing Research*, Vol. 13, No. 2, pp. 123-126, 2012.
- [12] Hemaunt Kumar, R. C. Srivastava, Puneet Negi, and H. M. Agrawal, "Effect of sintering temperature on the structural properties of cobalt ferrite nanoparticles," *Int. J. Materials Engineering Innovation*, Vol. 5, No. 3, pp. 227-238, 2014.
- [13] Partha P. Goswami, Hanif A. Choudhury, Sankar Chakma, and Vijayanand S. Moholkar, "Sonochemical synthesis of cobalt ferrite nanoparticles," *International Journal of Chemical Engineering*, Vol. 2013, pp. 1-6, 2013.
- [14] Mahmoud Goodarz Naseri, Elias B. Saion, Hossein Abbastabar Ahangar, Abdul Halim Shaari, and Mansor Hashim, "Simple synthesis and characterization of cobalt ferrite nanoparticles by a thermal treatment method," Vol.2010, No75, pp. 8, 2010.
- [15] J. Jiang and L. H. Ai, "Synthesis and characterization of Fe-Co binary ferrosipinel nanospheres via one-step nonaqueous solution pathway," *Materials Letters*, Vol. 64, No. 8, pp. 945-947, 2010.
- [16] Raming T.P., Winnubust A.J.A., Van Kats C.M., Philipse P., "The synthesis and magnetic properties of nanosized hematite particles," *J. Colloid Interface Sci.*, Vol. 249, No.2, pp. 346, 2002.
- [17] Sheena Xavier, Smitha Thankachan, Binu P. Jacob, and E.M. Mohammed, "Effect of sintering temperature on the structure and magnetic properties of cobalt ferrite nanoparticles," *Nanosystems: Physics, Chemistry, Mathematics*, Vol. 4, No. 3, pp. 430-437, 2013.
- [18] K.Maaz, Arif Mumtaz, S.K. Hasanain, and Abdullah Ceylan, "Synthesis and magnetic properties of cobalt ferrite ( $\text{CoFe}_2\text{O}_4$ ) nanoparticles prepared by wet chemical route," *J. M. & M. M.*, Vol.308, Issue 2, pp. 289-295, 2006.
- [19] S. Pauline and A. Pprysis Amalia, "Size and shape control evaluation of cobalt and cobalt ferrite ( $\text{CoFe}_2\text{O}_4$ ) magnetic nanoparticles," Vol. 3, N. 2, pp. 78-83, 2012.
- [20] Partha P. Goswami, Hanif A. Choudhury, Sankar Chakma, and Vijayanand S. Moholkar, "Sonochemical synthesis of cobalt ferrite nanoparticles," *International Journal of Chemical Engineering*, Vol. 2013, pp. 1-6, 2013.
- [21] A.E. Segneanu, P. Vlazan, P. Svera, I. Grozescu, and P. Sfirloaga, "Magnetic cobalt ferrite nanoparticles: synthesis and surface functionalization with naturally small peptide," *Digest Journal of Nanomaterials and Biostructures*, Vol. 9, No. 2, pp. 891 – 898, 2014.
- [22] A. Shutka, G. Mezinskis, and A. Pludons, "Preparation of dissimilarly structured ferrite compounds by sol-gel auto-combustion method," *CHEMINÉ TECHNOLOGIJA*, ISSN 1392 – 1231, Nr. 1, Vol. 54, pp. 41-46, 2010.